MICROBIOTA

Lung and gut microbiota are altered by hyperoxia and contribute to oxygen-induced lung injury in mice

Shanna L. Ashley[1], Michael W. Sjoding[1,2,3], Antonia P. Popova[4], Tracy X. Cui[4], Matthew J. Hoostal[5], Thomas M. Schmidt[5,6], William R. Branton[1], Michael G. Dieterle[5,6], Nicole R. Falkowski[1], Jennifer M. Baker[1,6], Kevin J. Hinkle[1], Kristine E. Konopka[7], John R. Erb-Downward[1], Gary B. Huffnagle[1,6,8,9], Robert P. Dickson[1,3,6]*

Inhaled oxygen, although commonly administered to patients with respiratory disease, causes severe lung injury in animals and is associated with poor clinical outcomes in humans. The relationship between hyperoxia, lung and gut microbiota, and lung injury is unknown. Here, we show that hyperoxia conferred a selective relative growth advantage on oxygen-tolerant respiratory microbial species (e.g., *Staphylococcus aureus*) as demonstrated by an observational study of critically ill patients receiving mechanical ventilation and experiments using neonatal and adult mouse models. During exposure of mice to hyperoxia, both lung and gut bacterial communities were altered, and these communities contributed to oxygen-induced lung injury. Disruption of lung and gut microbiota preceded lung injury, and variation in microbial communities correlated with variation in lung inflammation. Germ-free mice were protected from oxygen-induced lung injury, and systemic antibiotic treatment selectively modulated the severity of oxygen-induced lung injury in conventionally housed animals. These results suggest that inhaled oxygen may alter lung and gut microbial communities and that these communities could contribute to lung injury.

INTRODUCTION

Elemental oxygen is vital for human survival and plays an essential role in a diverse range of biological and physiological processes. Inhaled oxygen is widely used therapeutically in the treatment of acute and chronic hypoxemia. Yet, hyperoxia—elevated inhaled oxygen—causes lethal lung injury in animals (*1*–*3*), and in humans, it is associated with increased mortality (*4*, *5*), severe lung injury (*2*, *6*), and pneumonia (*7*, *8*). The injurious effects of hyperoxia on lung biology are well established, and the effects are robust across mammalian species (*1*, *9*, *10*). Yet, the mechanisms by which hyperoxia provokes diffuse lung alveolar inflammation and injury remain incompletely understood (*2*, *11*). In addition, the variations in susceptibility of individuals to oxygen-induced lung injury are incompletely explained by genetic variation (*12*–*14*).

Recent advances in culture-independent microbiology have revealed that the lungs, previously considered sterile, harbor complex and dynamic communities of bacteria (*15*). The lung microbiota are detectable in health (*16*–*18*), are altered in disease (*19*, *20*), correlate with variation in airway and alveolar immunity (*16*, *18*, *21*), and are predictive of clinical outcomes (*22*–*24*). Lung-associated bacteria vary widely in their tolerance of oxidative stress, and lung microbiota are profoundly altered in patients with respiratory failure receiving high concentrations of therapeutic oxygen (*21*, *25*). Although conditions of environmental hyperoxia are uncommon outside of patients' airways and alveoli, oxidative stress is a crucial determinant of bacterial community structure (*26*–*29*). Lung-associated bacteria vary profoundly in their tolerance of oxidative stress, ranging from obligate anaerobes (e.g., *Prevotella* spp.) to facultative anaerobes (e.g., *Pseudomonas aeruginosa*) to obligate aerobes (e.g., *Mycobacteria tuberculosis*). *Staphylococcus aureus*, the most common pathogen in ventilator-associated pneumonia (*30*), has evolved numerous mechanisms for enduring oxidative stress (*31*). Conditions of lung inflammation are characterized by high oxidative stress (*32*), given that a key feature of the innate immune response is the generation of reactive oxygen species and reactive nitrogen species by inflammatory cells of the immune system (*33*). Thus, mechanistic overlap likely exists in the adaptive strategies of respiratory pathogens such that they can survive both the innate immune response and environmental hyperoxia. In addition, gut microbiota have been implicated in patient susceptibility to pneumonia (*34*, *35*). The ecological effects of hyperoxia on lung and gut microbiota are unknown, as is the biological importance of oxygen-induced disruption of lung and gut microbiota.

We demonstrate here that lung and gut microbiota play a causal role in the pathogenesis of oxygen-induced lung injury in mice. Acute hyperoxia altered the bacterial community composition of murine lung and gut microbiota, selectively favoring the enrichment of oxygen-tolerant taxa in the lungs (e.g., *Staphylococcus* spp.). Oxygen-induced lung dysbiosis temporally preceded the development of lung injury, and among genetically identical mice with the same duration of hyperoxia exposure, variations in lung and gut microbiota correlated with variations in the severity of lung inflammation. Germ-free mice were protected from oxygen-induced lung injury, and systemic antibiotic treatment of conventionally housed mice selectively modulated susceptibility to oxygen-induced lung injury. We further demonstrated with in vivo and ex vivo mouse models that

[1]Division of Pulmonary and Critical Care Medicine, Department of Internal Medicine, University of Michigan Medical School, Ann Arbor, MI, USA. [2]Department of Computational Medicine and Bioinformatics, University of Michigan Medical School, Ann Arbor, MI, USA. [3]Michigan Center for Integrative Research in Critical Care, Ann Arbor, MI, USA. [4]Division of Pediatric Pulmonology, Department of Pediatrics, University of Michigan Medical School, Ann Arbor, MI, USA. [5]Department of Internal Medicine, University of Michigan Medical School, Ann Arbor, MI, USA. [6]Department of Microbiology and Immunology, University of Michigan Medical School, Ann Arbor, MI, USA. [7]Department of Pathology, University of Michigan Medical School, Ann Arbor, MI, USA. [8]Department of Molecular, Cellular, and Developmental Biology, University of Michigan, Ann Arbor, MI, USA. [9]Mary H. Weiser Food Allergy Center, University of Michigan, Ann Arbor, MI, USA.
*Corresponding author. Email: rodickso@med.umich.edu

the altered microenvironment of the oxygen-injured lung was more conducive to the growth of oxygen-enriched taxa such as *S. aureus*.

RESULTS

Hyperoxia exposure predicts subsequent bacterial growth from patient respiratory specimens

To address how hyperoxia may affect the lung microbiota, we first studied a cohort of critically ill patients to determine whether exposure to therapeutic oxygen influenced the respiratory microbiota identified using conventional culture of patient respiratory specimens. We analyzed clinical and microbiological data from hospitalized patients at the University of Michigan Hospital. We included in our analysis adult patients admitted to the intensive care unit (ICU) over a 4-year period (2015 to 2018) who received mechanical ventilation for greater than 24 hours and who had a respiratory specimen collected for bacterial culture during the subsequent 6 days (n = 1523). We stratified patients according to early hyperoxia exposure, which was calculated using the mean FiO_2 (fraction of inspired oxygen) delivered during the first 24 hours of the patient's admission. Patients were stratified into tertiles: low (FiO_2 21 to 46%), intermediate (FiO_2 43 to 55%), and high (FiO_2 >55%) hyperoxia exposure. We compared these tertiles and correlated them with the identity of bacteria grown from the patients' respiratory specimens and with the rate of isolation of specific bacterial species (Fig. 1).

We found marked differences in the bacterial species cultured from the lungs of patients who received low, intermediate, or high FiO_2 early in their ICU stay (Fig. 1A). Patients in the low FiO_2 tertile had comparable percentages of *S. aureus* and *P. aeruginosa* identified in subsequent positive cultures of their respiratory specimens (28.3 and 22.6%, respectively). In contrast, respiratory specimens from patients in the high FiO_2 tertile when cultured yielded twice as many *S. aureus* isolates compared to *P. aeruginosa* isolates (35.9 versus 14.9%, respectively). Given this apparent oxygen-associated difference between *S. aureus* and *P. aeruginosa*, the two most common pathogens in ventilator-associated pneumonia (*30*), we performed separate regression analyses to determine the relationship between hyperoxia and subsequent culture growth of these two bacterial species. We hypothesized that *S. aureus* and *P. aeruginosa*, which differ physiologically in their capacity to tolerate oxidative stress (*31*, *36*), would similarly differ in their resilience to hyperoxia in the lungs of critically ill patients. Given the multiple potential confounders in this complex patient population, we controlled for age, sex, race, antibiotic treatment (anti-staphylococcal and anti-pseudomonal), severity of illness (Sequential Organ Failure Assessment or SOFA score), and the number of respiratory cultures acquired per patient.

We found a significant association between early oxygen exposure and the identity of subsequently cultured respiratory bacteria (Fig. 1A). Rates of *P. aeruginosa* isolation were higher among patients receiving low and intermediate concentrations of FiO_2 (8.6 and 7.6%, respectively) relative to patients receiving high concentrations of FiO_2 (3.6%) (P = 0.001 and P = 0.007, respectively). In contrast, rates of *S. aureus* growth were not significantly different among patients receiving low, intermediate, or high concentrations of FiO_2 (P > 0.05 for all comparisons). We thus concluded that exposure to hyperoxia independently predicted subsequent bacterial growth from the lungs of critically ill patients, with differential species-specific effects. Specifically, rates of isolation of *S. aureus* from respiratory specimens were not affected by early exposure of critically ill patients to hyperoxia, whereas rates of *P. aeruginosa* isolation decreased among patients receiving high concentrations of FiO_2.

Hyperoxia disrupts the establishment of the lung microbiota in newborn mice

Given our observational human data suggesting that hyperoxia alters the lung microbiota, we next sought to model in vivo the ecological effects of hyperoxia on lung bacterial communities in mice. We sought to determine the acute effects of hyperoxia on both the establishment and disruption of the lung microbiota in newborn mouse pups, which are born without detectable lung bacteria (*37*, *38*).

To determine the effects of hyperoxia on the establishment of the lung microbiota in newborn mice, we used a well-established model of neonatal oxygen exposure (*39*). We randomly segregated newborn mouse pups (C57BL/6) from their common litters and exposed them to either hyperoxia (FiO_2 75%, n = 9) or normoxia (FiO_2 21%, n = 8) for 2 weeks and then characterized the lung microbiota using 16*S* ribosomal RNA (rRNA) gene sequencing. Compared to the lungs of normoxia-exposed mice, lungs of hyperoxia-exposed mice had decreased community richness (number of unique bacterial taxa for a given depth of sequencing) (P = 0.03; Fig. 1B). Hyperoxia had a large effect on the community composition of lung bacteria (P = 0.007; Fig. 1B). As identified by *mvabund* and BiPlot analysis, this difference was driven by the elimination of a prominent Erysipelotrichaceae taxon (P = 0.0004; Fig. 1B). This Erysipelotrichaceae taxon was the most abundant anaerobe in the lungs of normoxia-exposed mice, yet was not detected in hyperoxia-exposed mice. The Erysipelotrichaceae family has previously been reported in mice to be enriched by a low-fiber diet (*40*), associated with an allergic airway phenotype (*40*), and correlated with lung concentrations of interleukin-4 (IL-4) (*16*). In contrast, hyperoxia-exposed mice had increased relative abundance of an oxygen-tolerant *Streptococcus* species (P = 0.02; Fig. 1B).

Hyperoxia disrupts the established lung microbiota in adult mice

Having determined that hyperoxia affected the establishment of the lung microbiota in neonatal mice, we next asked whether acute hyperoxia disrupted the established lung microbiota in adult mice. We exposed genetically identical (C57BL/6) mice to various durations of acute hyperoxia (FiO_2 95%, n = 5 mice per time point) and then characterized lung microbiota using 16*S* rRNA gene sequencing and droplet digital polymerase chain reaction (ddPCR) quantification of the bacterial 16*S* gene. Acute hyperoxia altered the bacterial community composition of the lung microbiota of adult mice (P = 0.0064; Fig. 1C). Lung bacterial communities of hyperoxia-exposed mice exhibited a rapid and persistent decrease in relative abundance of prominent anaerobic taxa (e.g., the Clostridia and Bacteroidia classes; Fig. 1C). In contrast, the oxygen-tolerant *Staphylococcus* family surged in relative abundance after 72 hours of hyperoxia (P = 0.0007; Fig. 1C). The *Staphylococcus* family represented only 2.74% of all bacterial sequences in the lungs of normoxia-exposed mice, compared to 49.5% of all bacterial sequences in the lungs of mice exposed to 72 hours of hyperoxia. Rank abundance analysis of hyperoxia's effect on the lung microbiota is provided in fig. S1. The total bacterial burden in the lungs of hyperoxia-exposed mice did not change with duration of hyperoxia exposure (Fig. 1C), confirming that these observed bacterial community changes represented shifts in relative abundance rather than overgrowth by a dominant

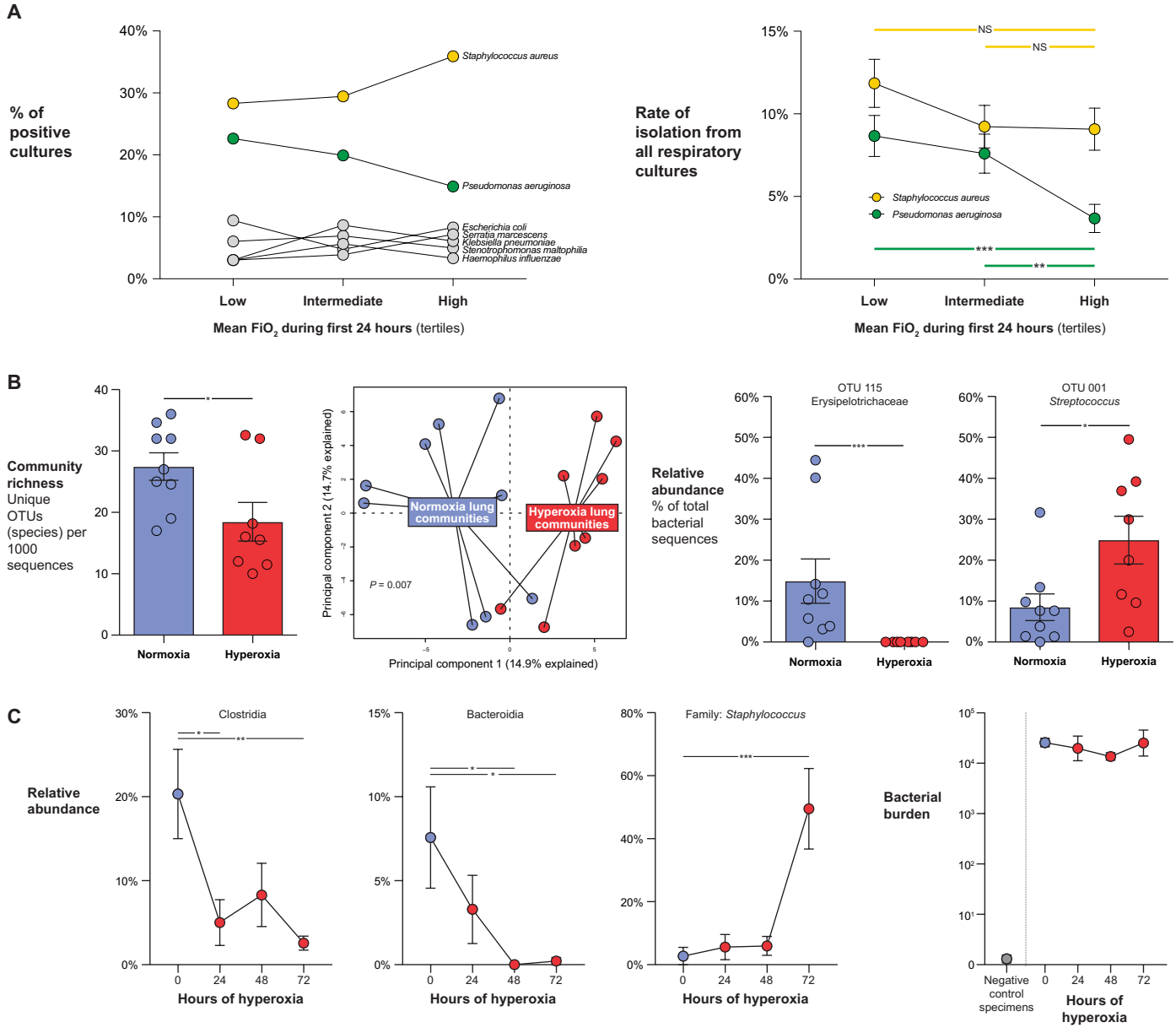

Fig. 1. Hyperoxia alters lung microbiota in humans and in neonatal and adult mice. (**A**) Comparison of early exposure to inhaled oxygen (FiO_2) in a cohort of 1523 patients receiving mechanical ventilation for greater than 24 hours and subsequent culture of respiratory specimens. Patients were stratified into tertiles by their mean FiO_2 during their first 24 hours of mechanical ventilation: low (FiO_2 21 to 46%; 265 isolates from 507 patients), intermediate (FiO_2 46 to 60%; 231 isolates from 508 patients), and high (FiO_2 60 to 100%; 181 isolates from 508 patients). (Left) The relationship between early hyperoxia (mean FiO_2 exposure during the first 24 hours) and the identity of bacterial species cultured from respiratory specimens in the week after collection is shown. (Right) The relationship between early hyperoxia and the rate of isolation of *S. aureus* and *P. aeruginosa* from all respiratory specimens sent for culture in the week after collection is shown. (**B**) (Left) Lung microbial community richness (measured as unique OTUs per 1000 sequences) compared across neonatal mice exposed to 2 weeks of normoxia (FiO_2 21%, $n = 8$) or hyperoxia (FiO_2 75%, $n = 9$) is shown. (Middle and right) Comparison of community composition of lung bacterial communities in neonatal mice exposed for 2 weeks to hyperoxia (FiO_2 75%, $n = 9$) or normoxia (FiO_2 25%, $n = 8$). (**C**) Relative abundance (percentage of total bacterial sequences) and bacterial burden (16*S* rRNA gene copies per lung) of lung microbiota of adult mice exposed to hyperoxia (FiO_2 95%, $n = 20$) for different time periods. Significance was determined by multivariable logistic regression (A), Mann-Whitney test (B), PERMANOVA (B), and ANOVA with Dunnet's test for multiple comparisons (C). Values represent means ± SEM. $*P \leq 0.05$; $**P \leq 0.01$; $***P \leq 0.001$. NS, not significant.

pathogen (as in acute staphylococcal pneumonia). We thus concluded that hyperoxia altered the establishment of the lung microbiota in newborn mice and disrupted the existing lung microbiota of adult mice, selectively enriching it with oxygen-tolerant taxa (e.g., *Staphylococcus* spp.).

Oxygen-induced lung microbiota dysbiosis precedes peak lung injury

Having determined that hyperoxia altered the mouse lung microbiota, we next sought to determine the relative timing of oxygen-induced dysbiosis and lung injury. It has been previously demonstrated that

lung injury itself is associated with an altered lung microbiota (*21*, *25*, *41*), presumably in part due to the altered microecology of the injured respiratory tract (*42*). We thus asked whether oxygen-induced disruption of lung microbiota preceded oxygen-induced lung injury, consistent with a causal role for the lung microbiota in pathogenesis, or whether dysbiosis followed lung injury, suggesting instead that lung microbiota disruption was merely an epiphenomenon of lung injury.

We compared the relative timing of lung microbiota disruption with that of lung injury during acute hyperoxia in adult mice. Consistent with prior studies, we found that detectable lung injury did not occur until after 72 hours of acute hyperoxia (FiO_2 95%) (P = 0.0001; Fig. 2A). By contrast, the lung bacterial communities of hyperoxia-exposed mice were altered after only 24 hours of hyperoxia (P = 0.0001; Fig. 2B). The rapid drop in prominent anaerobic taxa such as the Clostridia and Bacteroidia classes (Fig. 1C) demonstrated the rapidity of this shift in bacterial community composition. We thus concluded that oxygen-induced lung microbiota dysbiosis temporally preceded the onset of detectable lung injury, indicating that this disruption of the lung microbiota was not merely a consequence of an already-established lung injury.

In oxygen-exposed mice, variation in lung inflammation correlates with variation in lung microbial communities

Having determined that disruption of lung microbiota preceded lung injury in oxygen-exposed mice, we next sought to determine whether variation in oxygen-induced lung inflammation correlated with variation in lung microbiota. We have recently demonstrated that in healthy, genetically identical adult mice, variation in baseline immune tone (e.g., lung IL-1α) reflects variation in lung microbiota (*16*). For the current study, we analyzed large numbers of genetically identical mice (42 mice per time point) and ensured microbiological variation within each group by obtaining them from different vendors and shipments (*16*). At each time point, we compared the lung microbiota (characterized by 16*S* rRNA gene sequencing) with lung concentrations of key inflammatory cytokines, including IL-1α, a cytokine involved in pulmonary microbial surveillance (*16*, *43*, *44*), and tumor necrosis factor–α (TNF-α) and IL-17. Both TNF-α and IL-17 have been implicated in the pathogenesis of lung injury (*45*–*48*) and have been correlated with variation in the lung microbiota in humans (*18*, *21*).

As we have previously reported (*16*), lung concentrations of IL-1α varied inversely with the community diversity of lung bacteria in healthy adult mice [P = 0.0005, R^2 (coefficient of determination) = 0.2760; Fig. 3]. Yet, after 24 hours of hyperoxia (FiO_2 95%), this correlation was weakened (P = 0.0213, R^2 = 0.1351), and after 48 hours of hyperoxia, lung bacterial diversity and lung IL-1α concentrations were unrelated ($P > 0.05$, R^2 = 0.024). Thus, the correlation between lung microbiota diversity and lung IL-1α concentration was strongest in health and weakened with increasing duration of hyperoxia. In contrast, TNF-α and IL-17 exhibited the opposite trend with duration of hyperoxia (Fig. 3). In the lungs of unexposed mice, neither cytokine was detectable. After 24 hours of hyperoxia, both cytokines were detectable but were uncorrelated with lung bacterial diversity ($P > 0.05$ for both). Yet, after 48 hours of hyperoxia, both cytokines were detectable and inversely correlated with lung bacterial diversity (TNF-α: P = 0.0013, R^2 = 0.2350; IL-17: P = 0.0012, R^2 = 0.2372; Fig. 3). Variation in lung bacterial diversity explained greater than 23% of the variation in concentrations of both inflammatory cytokines after hyperoxia exposure.

We next compared the community composition of lung bacteria with variation in lung cytokines (fig. S2) and found a similar temporal trend. Among healthy, unexposed adult mice, variation in lung IL-1α concentration correlated significantly with the community composition of lung bacteria (P = 0.001) (fig. S2). This correlation weakened with duration of hyperoxia (24 hours P = 0.015, 48 hours P = 0.049). In contrast, variations in lung TNF-α and IL-17 concentrations were both significantly correlated with lung bacterial community composition at 24 hours (P = 0.004 for both) and 48 hours of hyperoxia (P = 0.015 and P = 0.008, respectively) (fig. S2A). No single taxonomic group was responsible for the correlation between lung bacterial communities and lung cytokine concentrations, indicating a complex community effect rather than a direct effect of a single bacterial species. Presence of the inflammation-associated Erysipelotrichaceae family was nominally associated with increased concentrations of IL-17 at both 24 and 48 hours of hyperoxia (fig. S2B). Correlations between lung bacterial taxa and lung concentrations of TNF-α and IL-17 (determined via *mvabund*) are shown in table S1. We concluded that among hyperoxia-exposed mice with identical genetics and duration of oxygen exposure, variation in lung inflammation correlated with variation in lung microbial communities.

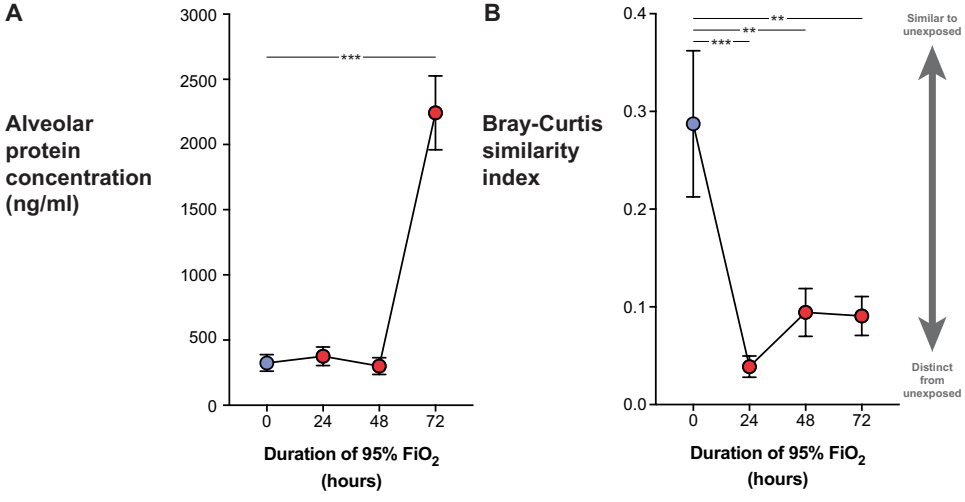

Fig. 2. Lung microbial dysbiosis precedes lung injury during hyperoxia in mice. Genetically identical adult mice were exposed to various durations of hyperoxia (FiO_2 95%, n = 20), and the temporal dynamics of lung injury and lung microbiota disruption were compared. (**A**) Alveolar protein concentration, a measure of lung injury, was compared to duration of hyperoxia. (**B**) Disruption of lung microbiota was measured using dissimilarity of lung microbial communities (Bray-Curtis similarity index) from those of mice unexposed to hyperoxia (time 0). Significance was determined using ANOVA with Dunnet's test of multiple comparisons. Values represent means ± SEM. $^{**}P \leq 0.01$; $^{***}P \leq 0.001$.

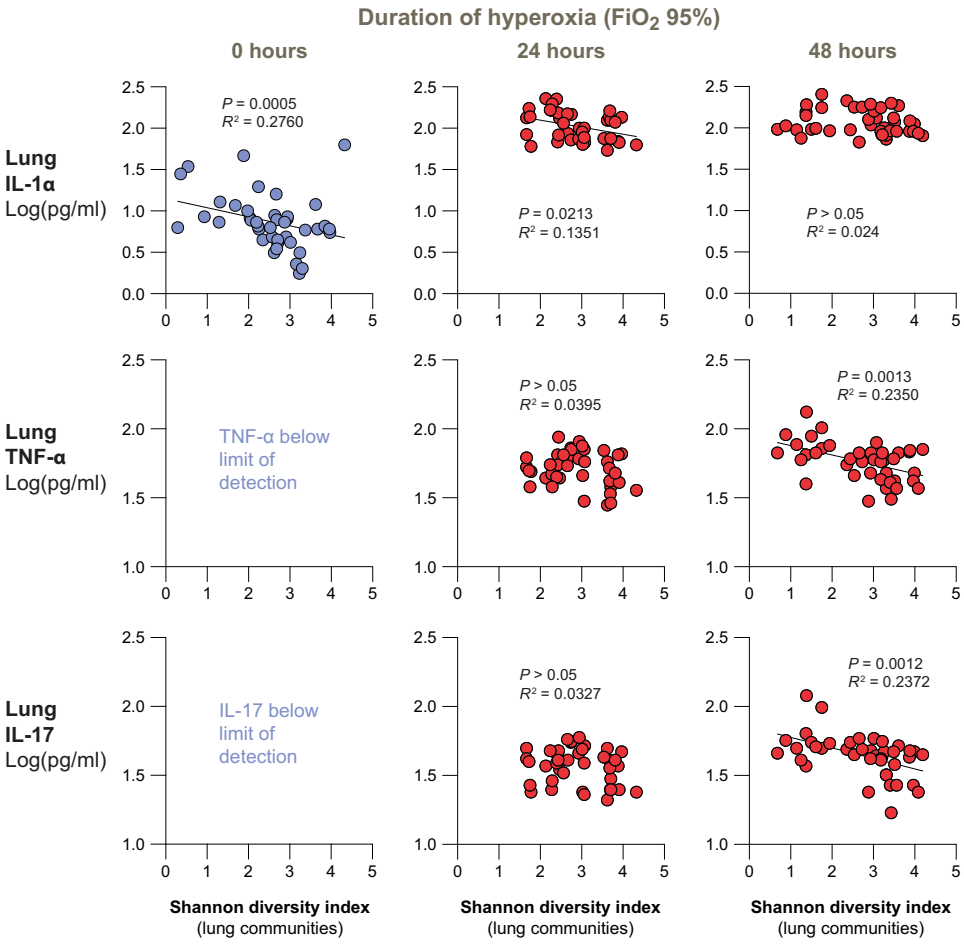

Fig. 3. Variation in lung inflammation correlates with variation in lung microbiota in hyperoxia-exposed mice. Healthy adult C57BL/6 mice were exposed to hyperoxia for 0, 24, and 48 hours (FiO_2 95%, $n = 42$ per time point). Variation in lung bacterial diversity (Shannon diversity index) was compared to concentrations of the cytokines IL-1α, TNF-α, and IL-17 at each time point. Significance was determined by linear regression using log-transformed cytokine data.

Gut bacterial communities are altered by hyperoxia and correlate with lung inflammation

Having established that acute hyperoxia alters lung microbial communities in adult mice and that early and late variation in lung immune tone correlated with variation in lung microbial composition and diversity, we next asked whether acute hyperoxia could alter the community composition of gut bacteria. To accomplish this, we exposed genetically identical (C57BL/6) mice to various durations of acute hyperoxia (FiO_2 95%, $n = 10$ mice per time point) and then characterized cecal bacteria using 16*S* rRNA gene sequencing. Duration of hyperoxia had a significant effect on the community composition of gut bacteria ($P = 0.005$; Fig. 4A), although this effect was not statistically significant until after 72 hours of hyperoxia ($P = 0.001$). No significant difference in gut microbial communities was detectable at shorter durations of hyperoxia (24 hours, $P = 0.315$; 48 hours, $P = 0.592$). The difference in community composition at 72 hours of hyperoxia was driven by relative depletion of the Firmicutes phylum and relative enrichment of the Bacteroidetes phylum ($P = 0.013$ for both; Fig. 4A). Hyperoxia-exposed mice showed significant depletion of the Ruminococcaceae family at 72 hours ($P = 0.021$). Hyperoxia had no significant effect on the community diversity of cecal communities ($P > 0.05$).

We next asked whether variation in gut bacterial communities could explain variation in lung inflammation in hyperoxia-exposed mice. We exposed genetically identical mice (42 mice per time point) to hyperoxia (95% FiO_2 for 24 and 48 hours) and compared the diversity and composition of cecal bacterial communities with inflammatory cytokine concentrations in lung (Fig. 4B). After 24 hours of hyperoxia, diversity of cecal bacterial communities did not correlate with lung concentrations of TNF-α and IL-17 ($P > 0.05$ for both; Fig. 4B). Yet, at 48 hours of hyperoxia, diversity of cecal communities did positively correlate with lung concentrations of TNF-α ($P = 0.0039$, $R^2 = 0.194$) and IL-17 ($P = 0.0008$, $R^2 = 0.254$). We found a similar temporal trend in our analysis of the community composition of cecal bacteria and lung cytokine concentrations (fig. S2A). The composition of cecal bacterial communities was unrelated to lung TNF-α and IL-17 concentrations after 24 hours of hyperoxia ($P > 0.05$ for both) but did correlate with both cytokines after 48 hours of hyperoxia ($P = 0.002$ for both; fig. S2A). Enrichment of cecal microbial communities with the Lachnospiraceae and Ruminococcaceae families was correlated with increased lung concentrations of TNF-α and IL-17 ($P < 0.001$; fig. S2C). Correlations between cecal bacterial taxa and lung concentrations of TNF-α and IL-17 (determined via *mvabund*) are shown in table S2.

Germ-free mice are protected from oxygen-induced lung injury

Having determined that lung and gut microbiota are altered by hyperoxia and that oxygen-induced dysbiosis preceded lung injury and correlated with lung inflammation, we next sought to determine whether the microbiota play a causal role in the pathogenesis of oxygen-induced lung injury or whether it was merely an epiphenomenon of lung injury. To accomplish this, we compared the effects of acute oxygen exposure in mice with conventional microbiota and experimentally manipulated microbiota, using germ-free mice, broad enteric antibiotics, or selective systemic antibiotics. We first compared mice with conventional microbiota to germ-free mice.

We exposed genetically identical (C57BL/6) germ-free mice and mice with a conventional microbiota to 72 hours of hyperoxia (FiO_2 95%, $n = 10$ mice per exposure per time point). Among mice with conventional microbiota, oxygen exposure provoked diffuse lung alveolar injury with increased concentrations of alveolar protein ($P = 0.0018$; Fig. 5A). By contrast, the lungs of hyperoxia-exposed

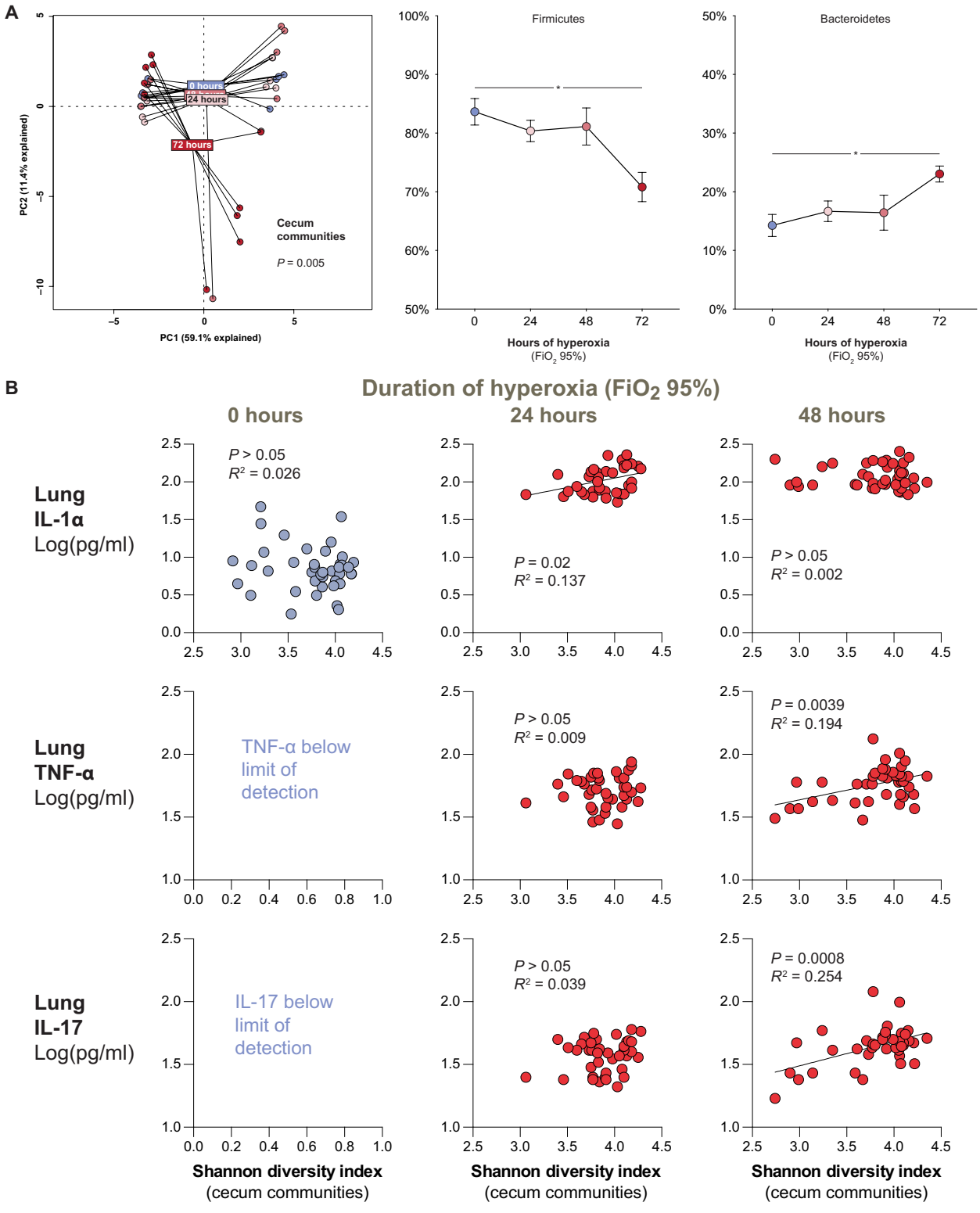

Fig. 4. Correlations among hyperoxia, cecal microbiota composition, and alveolar inflammation. Healthy, adult C57BL/6 mice were exposed to hyperoxia for 0, 24, 48, or 72 hours (FiO_2 95%). (**A**) Changes in cecal bacterial communities after exposure of mice to hyperoxia (FiO_2 95%, $n = 10$ per time point) for 72 hours reveal depletion of the Firmicutes phylum and enrichment of the Bacteroidetes phylum. PC1, principal component 1; PC2, principal component 2. Values represent means ± SEM. (**B**) Changes in cecal bacterial communities (Shannon diversity index) were compared with variations in lung inflammation measured by changes in the concentrations of the cytokines IL-1α, TNF-α, and IL-17 after 0, 24, or 48 hours of exposure to hyperoxia (FiO_2 95%, $n = 42$ mice per time point). Significance was determined via PERMANOVA (A), *mvabund* (B), and linear regression using log-transformed cytokine data (B).

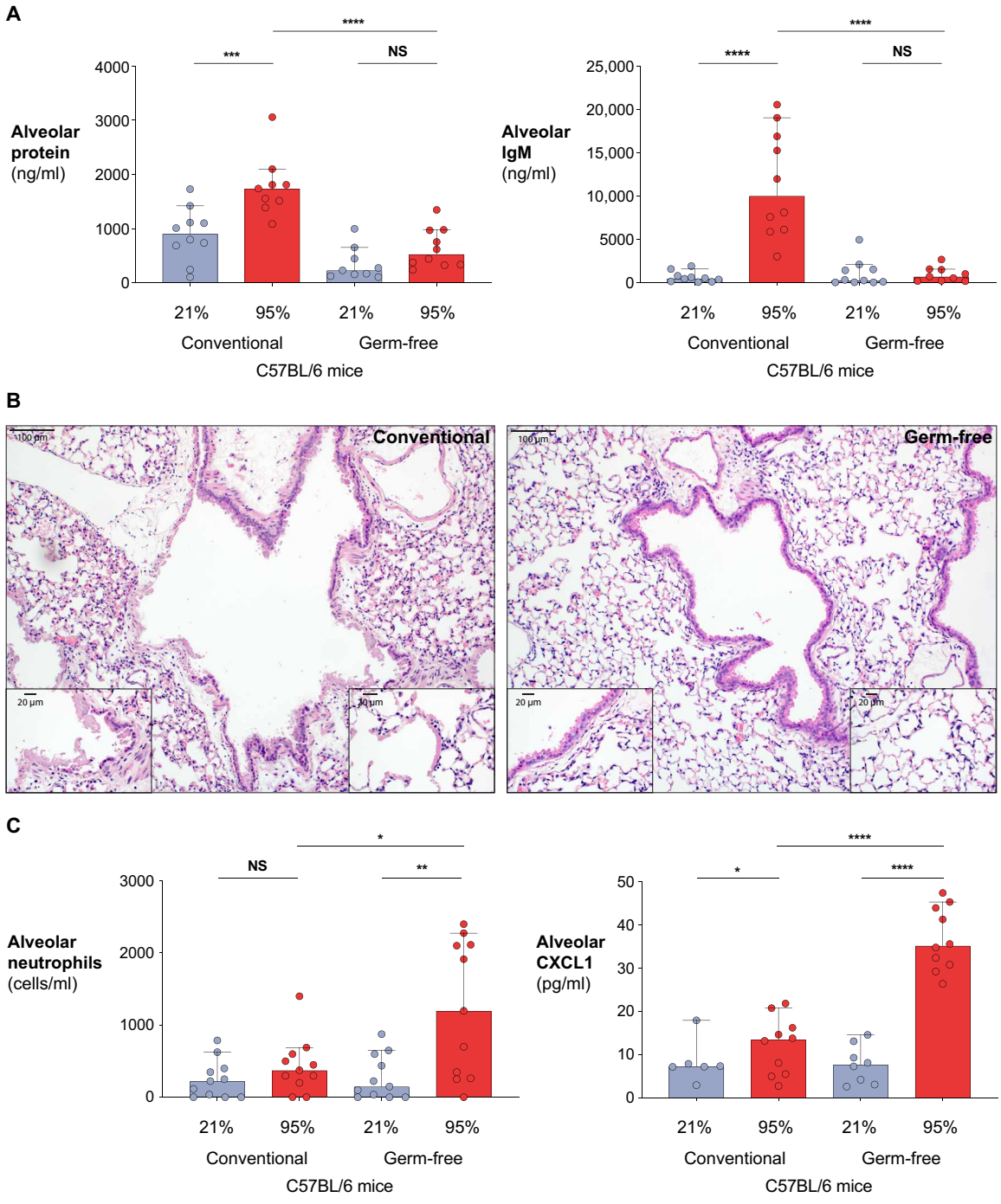

Fig. 5. Germ-free mice are protected from oxygen-induced lung injury. Conventionally housed (conventional) and germ-free C57Bl/6 adult mice were exposed to normoxia or hyperoxia (FiO_2 21 or 95%, respectively) for 72 hours, and oxygen-induced lung injury and alveolar inflammation were quantified. (**A**) Lung injury was quantified by measuring concentrations of alveolar protein and IgM in the lungs, which indicate alveolar capillary permeability ($n = 10$ per exposure per time point). (**B**) Representative histological images of lung tissue stained with hematoxylin and eosin from conventional ($n = 20$) or germ-free ($n = 12$) C57Bl/6 adult mice exposed to hyperoxia (FiO_2 95%) for 96 hours are shown. Left insets show epithelial necrosis and the formation of hyaline membranes; right insets show minimal epithelial injury and an intact normal alveolar architecture. (**C**) Alveolar inflammatory cells (neutrophils) and the neutrophil chemoattractant CXCL1 were quantified in bronchoalveolar lavage fluid from germ-free or conventional C57Bl/6 adult mice exposed to normoxia or hyperoxia (FiO_2 21 or 95%, respectively) for 72 hours. Significance was determined using Student's *t* test in (A) and (C). Values represent means ± SEM. $^*P \leq 0.05$; $^{**}P \leq 0.01$; $^{***}P \leq 0.001$; $^{****}P \leq 0.0001$.

germ-free mice had no more alveolar protein than did those of normoxia-exposed germ-free mice ($P = 0.0793$; Fig. 5A). Lungs of hyperoxia-exposed germ-free mice had significantly less alveolar protein than did those of hyperoxia-exposed mice with conventional microbiota ($P < 0.0001$; Fig. 5A). To further confirm this finding, we measured lung alveolar concentrations of immunoglobulin M

(IgM), a serum macromolecule that enters the lung alveolae after injury to the alveolar-capillary barrier (*49*, *50*). Hyperoxia provoked elevated alveolar IgM concentrations in mice with conventional microbiota ($P < 0.0001$) but had no effect on germ-free mice ($P = 0.4967$) (Fig. 5A). When comparing hyperoxia-exposed mice, alveolar IgM was markedly higher in mice with conventional microbiota when compared to germ-free mice ($P < 0.0001$; Fig. 5A).

We next asked whether germ-free mice were protected from histological evidence of oxygen-induced lung injury. We exposed genetically identical (C57BL/6) mice with conventional microbiota or germ-free mice ($n = 20$ and 12, respectively) to various durations of hyperoxia (FiO_2 95%, 0 to 96 hours) and examined their lungs for evidence of epithelial injury. At time points 0, 24, 48, and 72 hours, we observed no histological evidence of lung injury in either group (conventional microbiota or germ-free) (Fig. 5B). At 96 hours of hyperoxia, the lungs of mice with conventional microbiota uniformly exhibited evidence of acute lung injury including diffuse epithelial necrosis with the presence of hyaline membranes (Fig. 5B). In contrast, the lungs of germ-free mice exposed to hyperoxia were uniformly normal in their alveolar architecture, with no evidence of epithelial injury or hyaline membrane formation (Fig. 5B). These results confirmed that germ-free mice were protected from oxygen-induced lung injury.

We then asked whether germ-free mice differed from mice with conventional microbiota in their alveolar inflammatory response to hyperoxia. When compared to mice with conventional microbiota, germ-free mice had increased alveolar neutrophilia, both when comparing the percentage of total alveolar cells ($P = 0.016$) and when comparing absolute alveolar neutrophil counts ($P = 0.004$; Fig. 5C). Given this finding, we measured alveolar concentrations of CXCL1, a key neutrophil chemoattractant that is elevated in oxygen-induced lung injury (*51*, *52*). We found that alveolar CXCL1 concentrations were elevated in oxygen-exposed germ-free mice compared to oxygen-exposed mice with conventional microbiota ($P < 0.0001$; Fig. 5C), paralleling the difference observed with alveolar neutrophilia.

Antibiotics modify mouse susceptibility to oxygen-induced lung injury

We next asked whether antibiotic administration, either enteric or systemic, influenced mouse susceptibility to oxygen-induced lung injury. For enteric antibiotics, we used a broad-spectrum regimen of four antibiotics (ampicillin, neomycin, metronidazole, and vancomycin), administered for 3 weeks via drinking water, that was previously shown to influence mouse susceptibility to pneumococcal pneumonia (*34*). For systemic antibiotics, we used two regimens with distinct and complementary spectra of coverage: vancomycin, which has activity against Gram-positive bacteria including *Staphylococcus*, and ceftriaxone, which has broad activity against Gram-negative bacteria (and limited Gram-positive coverage relative to vancomycin). We have previously demonstrated that systemic ceftriaxone has taxonomically predictable effects on the lung microbiota of healthy mice (*16*). Both systemic antibiotics are commonly used in hospitalized patients receiving inhaled oxygen.

We first determined the effects of broad enteric antibiotics on oxygen-induced lung injury and inflammation ($n = 10$ mice per exposure per time point). Enteric antibiotics, administered in drinking water for 3 weeks before oxygen exposure, had no effect on severity of lung injury as measured by alveolar protein ($P = 0.528$) or IgM ($P = 0.691$) (Fig. 6A). Yet, treatment with enteric antibiotics did result in increased alveolar neutrophilia in oxygen-exposed mice ($P = 0.006$; Fig. 6A), recapitulating the increased alveolar neutrophilia observed in oxygen-exposed germ-free mice.

We then administered systemic antibiotics using intraperitoneal administration of single agents with contrasting spectra of coverage that both have well-established penetration of the lung ($n = 10$ per exposure per time point). Antibiotics were administered intraperitoneally for every day of the oxygen exposure. Systemic vancomycin, which has broad Gram-positive coverage, had no effect on lung injury as measured by alveolar protein ($P = 0.756$) or IgM ($P = 0.973$) (Fig. 6B). Yet, systemic ceftriaxone, which has broad Gram-negative coverage, resulted in increased lung injury as measured by alveolar protein ($P = 0.0005$; Fig. 6C). To confirm this finding and better characterize the temporal dynamics of ceftriaxone's effect on lung injury, we repeated the experiment and quantified alveolar IgM at multiple time points between 0 and 96 hours of hyperoxia ($n = 80$ total mice, 5 mice per exposure per time point). Alveolar IgM increased in all hyperoxia-exposed mice (saline and ceftriaxone) at 72 hours of hyperoxia, with a further increase among the ceftriaxone-treated mice at 96 hours (Fig. 6C).

Direct effects of hyperoxia on the host alter microbial growth conditions in the lung microenvironment

As recently reported (*21*, *25*), the lung microbiota of individuals with severe lung injury (acute respiratory distress syndrome) are profoundly altered and correlate with alveolar inflammation. The alveolar ecosystem, normally inhospitable to bacterial reproduction (*17*), is radically altered by the features of lung injury (*42*). Such changes include nutrient-rich edema, a surge in bacterial growth-promoting inflammatory molecules (*53*), and impairment of host defenses (*42*, *54*, *55*). We thus asked whether the direct effects of hyperoxia on host biology could alter the ecological conditions of the lung microenvironment, independent of oxygen's differential effects on lung microbial growth.

To determine this, we exposed genetically identical (C57BL/6) mice to various durations of hyperoxia (FiO_2 95%, 0 to 48 hours) and then challenged their lungs by intranasal instillation of *S. aureus* [10^7 colony-forming units (CFU)]. Mice were then observed for 24 hours under normoxic conditions (FiO_2 21%, $n = 20$ mice across time points). Thus, any difference in *S. aureus* burden across experimental groups was attributable to the sequelae of hyperoxia rather than the direct ecological pressure of hyperoxia itself. As compared to unexposed mice, we found a significant and duration-dependent effect of hyperoxia on subsequent clearance of *S. aureus* in oxygen-exposed mice ($P \leq 0.0001$; Fig. 7A).

We next sought to determine whether this effect was solely attributable to the impaired immune defenses of the hyperoxia-exposed mouse host. We accomplished this by using an ex vivo culture model, in which sterilized bronchoalveolar lavage fluid was used as a culture medium for a fixed bacterial inoculum. Thus, any differences in bacterial growth promotion or inhibition across treatment groups were attributable to noncellular features of the lung microenvironment (e.g., nutrient availability or growth-promoting/inhibiting mediators). We exposed genetically identical adult mice to 72 hours of normoxia (FiO_2 21%) or hyperoxia (FiO_2 95%) and then compared their bronchoalveolar lavage fluids for the relative growth promotion or inhibition of an identical *S. aureus* inoculum in vitro ($n = 7$ mice per group). Compared to saline and lavage fluid from normoxia-exposed mice, lavage fluid from hyperoxia-exposed mice promoted

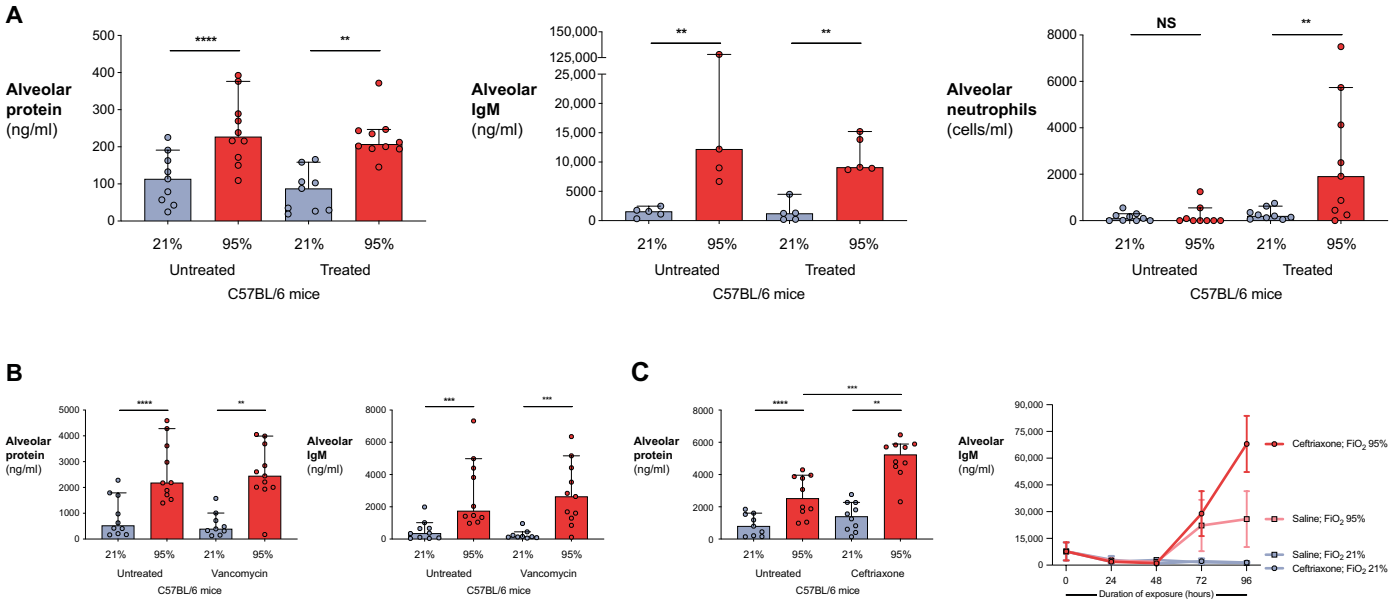

Fig. 6. The effects of antibiotic treatment on lung injury and inflammation in hyperoxia-exposed mice. (**A**) C57BL/6 conventionally housed adult mice were treated orally with broad-spectrum enteric antibiotics for 3 weeks (ampicillin, neomycin, metronidazole, and vancomycin) and then were exposed to normoxia (FiO_2 21%) or hyperoxia (FiO_2 95%) for 72 hours. Lung injury was quantified by measuring concentrations of alveolar protein and IgM as well as neutrophils in bronchoalveolar lavage fluid from antibiotic-treated and untreated mice. (**B** and **C**) C57BL/6 conventionally housed adult mice were treated daily with intraperitoneal vancomycin (B) or intraperitoneal ceftriaxone (C) during a 72-hour exposure to normoxia (FiO_2 21%) or hyperoxia (FiO_2 95%). Lung injury was quantified by measuring concentrations of alveolar protein and IgM in bronchoalveolar lavage fluid from antibiotic-treated and untreated mice. Significance was determined using Student's *t* test. Values represent means ± SEM. $^{**}P \leq 0.01$; $^{***}P \leq 0.001$; $^{****}P \leq 0.0001$.

the growth of *S. aureus* in culture ($P \leq 0.0001$ for both comparisons; Fig. 7B).

DISCUSSION

Here, we demonstrate that inhaled oxygen alters lung and gut microbiota of mice, selectively enriching lung bacterial communities with oxygen-tolerant taxa (e.g., *Staphylococcus* spp.) (fig. S3). During hyperoxia exposure, lung dysbiosis preceded lung injury and correlated with variation in severity of lung inflammation. Germ-free mice were protected from oxygen-induced lung injury, and systemic antibiotic treatment selectively modulated the severity of oxygen-induced lung injury. Further, the direct effects of hyperoxia on host biology altered the lung microenvironment, indirectly and selectively favoring enhanced bacterial growth. These findings suggest that lung microbiota contribute to the pathogenesis of lung injury in mice.

Before J. Priestley isolated and inhaled pure oxygen in 1774 (*10*), no environment on Earth had exceeded an oxygen concentration of 35% during the preceding 3.8 billion years of microbial evolution (*56*). Yet, because of the ubiquitous clinical use of inhaled oxygen, patients' airways and alveoli are routinely exposed to sustained oxygen concentrations between 30 and 100%. We demonstrate oxygen-induced dysbiosis in the lung environment, and our findings are consistent with prior evidence of oxygen's crucial role in determining microbial community structure (*26*, *28*, *29*). In environmental microbial communities, oxygen gradients exert profound effects on community structure (*26*, *29*). Within the human gut, the luminal gradient from hypoxia (10%) to anoxia (0%) plays a determinant role in community structure (*28*). When antibiotics deplete the gut's resident butyrate-producing Clostridia, butyrate-starved colonocytes revert to anaerobic glucose fermentation, increasing luminal oxygen concentrations and promoting expansion of the disease-associated Enterobacteriaceae family (*28*, *57*). While we observed a similar depletion of Clostridia in the lungs after hyperoxia, we found a relative expansion of the *Staphylococcus* family, consistent with the apparent resilience of *S. aureus* relative to other respiratory pathogens in hyperoxia-exposed humans (Fig. 1). Like most lung disease–associated bacteria (e.g., *P. aeruginosa* and *Streptococcus pneumoniae*), *S. aureus* has multiple, complementary mechanisms of coping with oxidative stress (*31*). *S. aureus* expresses detoxifying enzymes (e.g., superoxide dismutase) (*58*, *59*), catalase (*58*, *60*), flavohemoglobin (*61*), DNA protection enzymes and DNA repair enzymes [e.g., MrgA (*31*)], and protein damage repair enzymes (e.g., thioredoxin) (*62*). Given that a primary innate immune defense mechanism deployed by neutrophils (*63*) and alveolar macrophages (*64*) is an "oxidative burst" (the rapid release of reactive oxygen species), it is expected that lung-associated pathogens have evolved mechanisms for enduring oxidative stress.

An important and unresolved question is the relative contributions of local (lung) and remote (lower gut) bacterial communities to lung inflammation and injury. Although we have shown that manipulation of the microbiota can influence susceptibility to oxygen-induced lung injury (either via antibiotics or use of germ-free animals), it is unknown whether these effects are more attributable to the lung or gut microbiota. We have previously demonstrated that among genetically identical mice, variation in lung innate immunity more strongly reflects lung microbiota than gut microbiota (*16*).

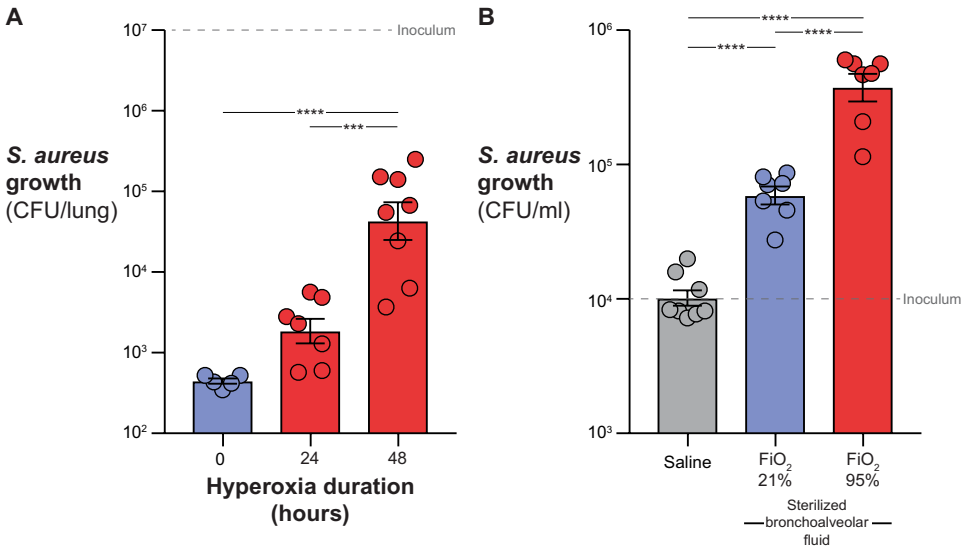

Fig. 7. Hyperoxia alters microbial growth conditions in the mouse lung microenvironment. (**A**) Conventionally housed C57Bl/6 adult mice were exposed to hyperoxia (95% FiO_2) for 0, 24, or 48 hours ($n = 20$ mice) and then were administered intranasal *S. aureus* (10^7 CFU). Thereafter, mice were observed for 24 hours at normoxia (21% FiO_2), after which their lungs were harvested, and *S. aureus* CFU were counted. (**B**) The mouse lung microenvironment was analyzed ex vivo by inoculating 10^4 CFU of *S. aureus* into saline as a control or sterilized bronchoalveolar lavage fluid from mice exposed to normoxia or hyperoxia for 72 hours. *S. aureus* CFU were then quantified after 6 hours of growth ($n = 7$ per exposure). Significance was determined using ANOVA with Bonferroni correction for multiple comparisons. Values represent means ± SEM. ***$P \leq 0.001$; ****$P \leq 0.0001$.

Human studies have revealed correlations between lung microbiota and lung immunity in health and disease (*18*, *21*, *24*, *65*). In our current study, variation in lung inflammation correlated with the diversity and community composition of lung and gut microbial communities, although correlation with lung microbial communities preceded correlation with gut microbial communities (24 versus 48 hours). Similarly, although hyperoxia altered both lung and gut microbial communities, the effects on the lung microbiota were more immediate (24 hours) than those on the gut microbiota (72 hours). Systemic antibiotic treatment (intraperitoneal ceftriaxone) with demonstrated effects on lung microbiota (*16*) modulated the severity of oxygen-induced lung injury, whereas enteric antibiotic treatment had no effect. We interpret these results as suggesting that microbiota in both lung and gut play important, temporally distinct roles in the pathogenesis of oxygen-induced lung injury, likely with lung bacteria informing the early response and gut bacteria informing the late response. Additional work will be necessary to determine the specific contributions of lung and gut microbiota to oxygen-induced lung injury.

Our study has several limitations. Whereas the injurious effects of profound hyperoxia (FiO_2 >95%) on lung biology are well established and uncontroversial, the biological and microbiological significance of the range of hyperoxia seen in routine clinical care is less established. Although the histology of our murine model of hyperoxia recapitulated the key features of human lung injury and the taxonomic changes observed in our oxygen-exposed mice aligned with those in our human cohort, there are important anatomic, immunologic, and microbiologic differences between mice and humans that will necessitate further validation. Last, our experimental approach did not let us selectively manipulate lung and gut microbiota in isolation to determine their relative importance in the pathogenesis of oxygen-induced lung injury.

Inhaled oxygen is arguably the most commonly administered therapy among hospitalized patients and is associated with increased mortality (*4*, *5*), severe lung injury (*2*, *6*), and pneumonia (*7*). Our study reveals that lung and gut dysbiosis may contribute to oxygen-induced lung injury. Further work is needed to identify (i) the mechanisms by which hyperoxia selectively enriches the lungs with aero-tolerant bacteria, (ii) the pathways by which oxygen-altered taxa promote and dampen alveolar inflammation, (iii) additional ecologic factors within injured lungs that promote and perpetuate bacterial growth, and (iv) the role of gastrointestinal microbiota in alveolar inflammation and injury. A better understanding of oxygen's role in homeostasis and its disruption at the host-microbiota interface may enable therapeutic modulation of the lung and gut microbiota for the prevention and treatment of oxygen-induced lung injury.

MATERIALS AND METHODS

Study design

We designed a series of complementary analyses and experiments to test the hypotheses that lung and gut microbiota are altered by inhaled oxygen and contribute to the pathogenesis of oxygen-induced lung injury. We first designed a retrospective observational cohort study of individuals with a prespecified comparison of culture-identified respiratory bacteria (outcome) stratified by early hyperoxia (predictor). We then designed prospective cohort studies in mice to determine whether a controlled exposure (hyperoxia) influenced the composition and identity of lung microbiota. We next designed a cross-sectional cohort study in mice to determine whether variation in lung and gut microbiota correlated with variation in lung inflammation after hyperoxia exposure. We then determined whether manipulation of gut and lung microbiota (using germ-free mice and antibiotics) altered the severity of oxygen-induced lung injury and inflammation in mice, as well as whether duration of hyperoxia exposure altered murine susceptibility to a model of *S. aureus* pneumonia. Randomization was used to assign mice to exposure and control arms for each experiment. Analysis of experimental murine data was not blinded.

All clinical investigations were conducted according to the principles of the Declaration of Helsinki. The institutional review board of the University of Michigan Health System (HUM00104714) approved the human study protocol. The deidentified analysis of patient data has been assessed to be no more than minimal risk with no need for a dedicated informed consent process. The institutional review board has examined the protocols and certified that "The risks are reasonable in relation to benefits to participants and the

knowledge to be gained. The risks of the study have been minimized to the extent possible."

The University Committee on the Care and Use of Animals at the University of Michigan (PRO00007791) approved the animal studies. Laboratory animal care policies at the University of Michigan follow the Public Health Service policy on Humane Care and Use of Laboratory Animals. Animals were assessed twice daily for physical condition and behavior. Animals assessed as moribund were humanely euthanized by CO_2 asphyxiation.

Human study population

The observational human cohort was identified via abstraction from the University of Michigan's electronic medical records. Inclusion criteria were (i) age ≥18 years; (ii) admission to the University of Michigan's Critical Care Medical Unit, Surgical Critical Care Unit, or Cardiac ICU between 1 January 2015 and 31 December 2018; (iii) mechanical ventilation for ≥24 hours; (iv) documentation of at least 10 FiO_2 measurements during the first 24 hours (for calculation of the mean FiO_2); and (v) respiratory culture performed between 24 hours and day 7 of hospitalization (i.e., subsequent to the FiO_2 exposure period). Early oxygen exposure was quantified by determining mean FiO_2 during the first 24 hours of hospitalization. Species-level taxonomic classification of cultured bacteria and fungi from respiratory specimens was determined by query of results reported by the University of Michigan Clinical Microbiology Laboratory. Respiratory specimens (bronchoalveolar lavage, miniature bronchoalveolar lavage, endotracheal aspirates, and sputum) were cultured according to standard clinical microbiology laboratory protocols.

Respiratory specimen culture

Respiratory specimens were cultured according to standard clinical microbiology laboratory protocols. Briefly, respiratory specimens were plated on chocolate, sheep blood, and MacConkey agar plates and incubated for 72 hours. Bacteria were identified and reported if they grew more than 10^4 CFU/ml or if they were under 10^4 CFU/ml but were a single Gram-negative bacillus and the only reportable pathogen. The following organisms, when identified, were reported as "oral flora": coagulase-negative *Staphylococcus* species (spp.), alpha-hemolytic *Streptococcus* spp., gamma-hemolytic *Streptococcus* spp., *Micrococcus* spp., *Enterococcus* spp., *Corynebacterium* spp., *Lactobacillus* spp., *Bacillus* spp. (other than *B. anthracis*), *Neisseria* spp., *Haemophilus* spp. (other than *H. influenzae*), *Eikenella* spp., *Capnocytophaga* spp., and yeast (other than *Cryptococcus* spp.). Detailed methods for electronic medical record chart abstraction and clinical microbiology protocols have been previously published (*66*, *67*). Analysis was performed using multivariable logistic regression. Covariates included age, sex, race, antibiotic exposure (anti-staphylococcal and anti-pseudomonal), severity of illness (SOFA score), and the number of respiratory cultures acquired.

Mice

Neonatal C57BL/6 mice were obtained from an in-house breeding colony (Fig. 1B). Nineteen pups from two litters were randomly assigned to hyperoxia (FiO_2 75%) or normoxia (FiO_2 21%) for 2 weeks. Mice were breastfed by the two litters' dams, which were rotated between environments every 48 hours. For initial acute hyperoxia exposures (Figs. 1C and 2), 8-week-old female C57BL/6 mice were purchased from the Jackson Laboratory (Bar Harbor, ME) and housed under specific pathogen–free conditions. Mice were housed in five animal cages and allowed to acclimate for 2 weeks before exposure and harvest at 10 weeks of age. For the heterogeneity analysis of lung microbiota and lung inflammation (Fig. 3), 8-week-old female C57BL/6 mice were purchased from the Jackson Laboratory (Bar Harbor, ME) and Charles River Laboratories (Wilmington, MA) and housed under specific pathogen–free conditions. Mice were treated in subsequent weeks over a 4-week period. Mice were housed and allowed to acclimate as previously mentioned. To avoid batch effect due to cohousing, mice from various cages were sampled at each time point in each experiment. Germ-free mice were obtained from the University of Michigan Germ-Free and Gnotobiotic Mouse Facilities. Ten-week-old C57BL/6 mice were used as germ-free and conventional microbiome controls in the germ-free comparison (Fig. 5A). Mice were housed in soft-sided plastic isolators, in which they remain free of all bacteria, exogenous viruses, fungi, and parasites, as determined by regular fecal monitoring and periodic control necropsies by both culture-based and PCR-based techniques. Data acquired from the unexposed mice (0 hours hyperoxia) in the heterogeneity of microbiota and inflammation experiment (Figs. 3 and 4B) have been reported in a previously published manuscript (*16*).

Enteric antibiotics: Mice were exposed to a previously published broad-spectrum regimen of enteric antibiotics as previously described (*34*). The following concentrations of antibiotics were administered via drinking water for 3 weeks before oxygen exposure: ampicillin (1 g/liter; Sigma-Aldrich), neomycin sulfate (1 g/liter; Sigma-Aldrich), metronidazole (1 g/liter; Sanofi-Aventis), and vancomycin (0.5 g/liter; Sandoz).

Systemic antibiotics: Ceftriaxone (ceftriaxone disodium salt C-5793, Sigma-Aldrich, St. Louis, MO) was administered at a dose of 50 mg/kg suspended in 200 μl of sterile water and administered intraperitoneally. Vancomycin (Sigma-Aldrich, St. Louis, MO) was administered at a dose of 20 mg/kg suspended in 200 μl of sterile water and administered intraperitoneally. For both systemic antibiotics, mice were exposed daily during the acute hyperoxia exposure (days 0, 1, and 2). Mice were removed from the oxygen chamber for 20 to 30 min during intraperitoneal administration of antibiotic or saline administration.

Hyperoxia exposure

Hyperoxia was administered to mice by placing their cages in a sealed chamber (BioSpherix) with medical-grade 100% oxygen (0.1 to 99.9 ± 0.1%) delivered continuously via a ProOx 110 oxygen controller to maintain chamber oxygen levels. Neonatal mice were administered FiO_2 75% for 2 weeks, based on an established model of bronchopulmonary dysplasia (*68*, *69*). Adult mice were administered FiO_2 95% for durations ranging from 24 to 96 hours. Germ-free mice were placed in the chamber using dedicated microisolator cages with sufficient food and water for the duration of exposure. Thus, microisolator cages were kept sealed and sterile until the time of tissue harvest.

Mouse tissue collection and processing

Mice were euthanized via CO_2 asphyxiation. Low biomass specimens (tongue, nasal rinse, and lung) were removed before high biomass specimens (cecum). Instruments were rinsed with ethanol and flamed between each organ. Murine lungs were excised, placed in tubes containing 1 ml of sterile water, and homogenized mechanically

by using a Tissue-Tearor (BioSpec Products, Bartlesville, OK). The tissue homogenizer was cleaned and rinsed in ethanol and water between each sample. Water control specimens from homogenization, exposed to cleaned instruments, were included in sequencing as procedural controls. For alveolar protein quantification, bronchoalveolar lavage was performed using 1 ml of phosphate-buffered saline instilled and aspirated into the surgically exposed trachea.

Bacterial DNA isolation

Genomic DNA was extracted from mouse tissue (Qiagen DNeasy Blood and Tissue kit, Qiagen, Hilden, Germany) and homogenized in PowerBead tubes (Qiagen, Hilden, Germany) using a modified protocol previously demonstrated to isolate bacterial DNA (*70*). Sterile laboratory water and AE buffer used in DNA isolation were collected and analyzed as potential sources of contamination. Specimens were processed in a randomized order to minimize the risk of false pattern formation due to reagent contamination (*71*).

16*S* rRNA gene sequencing

The V4 region of the 16*S* rRNA gene was amplified using published primers (*72*) and the dual-indexing sequencing strategy developed by the laboratory of P. D. Schloss (*73*). Sequencing was performed using an Illumina MiSeq platform (San Diego, CA), using the MiSeq Reagent Kit V2 (500 cycles), according to the manufacturer's instructions with modifications found in the Schloss standard operating procedure (*74*). AccuPrime High-Fidelity Taq was used in place of AccuPrime Pfx SuperMix. Primary PCR cycling conditions were at 95°C for 2 min, followed by 20 cycles of touchdown PCR (95°C for 20 s, 60°C for 20 s and decreasing 0.3°C each cycle, and 72°C for 5 min), then 20 cycles of standard PCR (95°C for 20 s, 55°C for 15 s, and 72°C for 5 min), and finished at 72°C for 10 min.

Bacterial DNA quantification

Bacterial DNA was quantified using a QX200 Droplet Digital PCR System (Bio-Rad, Hercules, CA). Primers and cycling conditions were performed according to a previously published protocol (*75*). Specifically, primers were 5′-GCAGGCCTAACACATGCAAGTC-3′ (63F) and 5′-CTGCTGCCTCCCGTAGGAGT-3′ (355R). The cycling protocol was 1 cycle at 95°C for 5 min, 40 cycles at 95°C for 15 s and 60°C for 1 min, 1 cycle at 4°C for 5 min, and 1 cycle at 90°C for 5 min—all at a ramp rate of 2°C/s. The Bio-Rad C1000 Touch Thermal Cycler was used for PCR cycling. Droplets were quantified using the Bio-Rad QuantiSoft software. Two replicates were used per sample. Negative control specimens were used and were run alongside lung specimens.

Protein and alveolar IgM quantification

Lung injury was assessed using quantification of total protein and IgM in bronchoalveolar lavage fluid. Bronchoalveolar lavage fluid was centrifuged for 30 min at 13,000 rpm. Protein was quantified colorimetrically using the Bradford assay (Bio-Rad, Hercules, CA). Alveolar IgM was quantified using the IgM Mouse Uncoated ELISA (enzyme-linked immunosorbent assay) Kit (Thermo Fisher Scientific, Waltham, MA).

Cytokine measurement

Cytokines were measured in whole lung homogenate according to the manufacturer's instructions using the following ELISA kits obtained from R&D Systems (Minneapolis, MN): Mouse IL-1α/IL-1F1 DuoSet ELISA DY400, Mouse IL-4 DuoSet ELISA DY404, Mouse TNF-α DuoSet ELISA DY410, Mouse IL-17 DuoSet ELISA DY421, and Mouse CXCL1/KC DuoSet ELISA DY453.

Identification of contaminants and adequacy of sequencing

In low-biomass microbiome studies, it is essential to determine the influence of contamination on sequencing results, as reagents used in DNA isolation and library preparation contain bacterial DNA that can contaminate sequencing-based studies of microbial communities (*71*). For each experiment using 16*S* rRNA gene sequencing, to identify potential sources of contamination in sequencing, we collected multiple procedural and sequencing control specimens. We included sterile water used in tissue collection (exposed to instruments used in harvesting and tissue homogenization), DNA extraction controls (empty bead tubes processed in parallel with tissue specimens), AE buffer used in DNA extraction, and blank wells in the MiSeq sequencing run. Mock community standards were analyzed as quality controls in each sequencing run, and samples were processed in a randomized manner to avoid batch effect from kit contamination.

For the neonatal hyperoxia exposure experiment (Fig. 1B), we sequenced 21 procedural control specimens: saline used in tissue harvest (3), water used in tissue homogenization (3), DNA extraction controls (empty bead tubes processed in parallel with tissue specimens) (4), sterile water used in DNA extraction (4), AE buffer used in DNA extraction (4), and mock community standards (3). We obtained 1,906,893 total reads for all tissue and control specimens (16,875 ± 19,945 per specimen). Two lung specimens (one hyperoxia-exposed and one normoxia-exposed) were excluded from analysis because of the small number of reads (60 and 40, respectively). Via permutational multivariate analysis of variance (PERMANOVA), we confirmed that bacterial taxa detected in negative control specimens were significantly distinct from taxa detected in lung, tongue, cecum, and colonic mucosa specimens ($P < 0.0001$ for all comparisons). The most prominent taxa detected in negative control specimens were OTU040:*Pelomonas*, OTU034:*Pseudomonas*, and OTU015: Porphyromonadaceae. These operational taxonomic units (OTUs) comprised 45.9% of all sequences detected in negative control specimens but comprised only 1.5% of sequences detected in lung specimens. No OTUs were excluded from analysis.

For the acute hyperoxia exposure in adult mice (Fig. 1C), we sequenced 48 negative control specimens: water used in tissue homogenization (5), DNA extraction controls (empty bead tubes processed in parallel with tissue specimens) (4), sterile water used in DNA extraction (2), AE buffer used in DNA extraction (6), blank MiSeq wells (31), and mock community standards (2). We obtained 1,425,377 total reads for all tissue and control specimens (20,362 ± 54,472 per specimen). No lung specimens were excluded from analysis. Via PERMANOVA, we confirmed that bacterial taxa detected in negative control specimens were significantly distinct from taxa detected in lung specimens ($P < 0.0001$). Communities were distinct both collectively and when stratified by duration of hyperoxia exposure ($P \leq 0.01$ for all comparisons). The most prominent taxa detected in negative control specimens were OTU002:Enterobacteriaceae, OTU031:*Pelomonas*, and OTU032:*Prevotella*. These OTUs comprised 54.0% of all the sequences detected in negative control specimens but comprised only 7.2% of the sequences detected in lung specimens. No OTUs were excluded from analysis.

For the heterogeneity of microbiota and lung immunity experiment (Figs. 4 and 5), we sequenced 96 negative control specimens: water used in tissue homogenization (12), DNA extraction controls

(empty bead tubes processed in parallel with tissue specimens) (18), sterile water used in DNA extraction (4), AE buffer used in DNA extraction (8), blank MiSeq wells (54), and mock community standards (4). We obtained 5,997,020 total reads for all tissue and control specimens (17,074 ± 23,929 per specimen). Via PERMANOVA, we confirmed that bacterial taxa detected in negative control specimens were significantly distinct from taxa detected in lung specimens ($P < 0.0001$). Communities were distinct both collectively and when stratified by duration of hyperoxia exposure ($P < 0.0001$ for all comparisons). A single OTU dominated negative control specimens, OTU003:Enterobacteriaceae_unclassified, comprising 31.9% of sequences in negative controls and 9.5% in lung specimens. This OTU was the most abundant taxon in all negative control types, even comprising 31.6% of sequences in blank MiSeq wells. This indicates that this OTU was actually not a contaminant introduced via reagents but instead noise-introduced during the sequencing process. The three most prominent taxa in negative control specimens were OTU003:Enterobacteriaceae_unclassified, OTU008:*Bacteroides*, and OTU045:*Flavobacterium*. These OTUs collectively comprised 38.9% of all sequences detected in negative control specimens and comprised 11.9% of sequences detected in lung specimens. No OTUs were excluded from analysis.

S. aureus instillation and cultivation

For the post-hyperoxia *S. aureus* clearance experiment (Fig. 7A), 10-week-old C57BL/6 mice were exposed to various durations of hyperoxia as detailed in Direct effects of hyperoxia on the host alter microbial growth conditions in the lung microenvironment and then challenged with intranasal instillation of *S. aureus*. A total of 10^7 CFU of a laboratory strain of *S. aureus* [USA300, Methicillin-resistant *Staphylococcus aureus* (MRSA)] were suspended in sterile saline and instilled under general anesthesia. Mice were then monitored for 24 hours under normoxic conditions (FiO_2 21%) and then harvested. Lung homogenate was plated on lysogeny broth (LB) agar plates for CFU determination and compared across treatment groups.

Ex vivo cultivation experiment

For the ex vivo cultivation experiment (Fig. 7B), 10-week-old C57BL/6 mice were exposed to normoxia (FiO_2 21%) or hyperoxia (FiO_2 95%) for 72 hours. Mice were then euthanized, and bronchoalveolar lavage was performed. Bronchoalveolar lavage fluid was sterilized via centrifugation (30 min at 30,000 rpm). Bronchoalveolar lavage fluid was passed through Amicon Ultra-0.5-ml Centrifugal filters (Millipore, Bedford, MA) and then divided into 100-μl aliquots and inoculated in duplicate with 10^4 CFU of *S. aureus* (USA300). Uninoculated aliquots were used as negative controls to confirm sterility of the fluid, with no detectable CFUs. After 6 hours of incubation at 37°C under normoxic conditions, each aliquot was then plated onto LB agar plates, and CFU were counted after 24 hours of subsequent growth.

Statistical analysis

Sequence data were processed and analyzed using the software mothur v.1.35.1 according to the standard operating procedure for MiSeq sequence data using a minimum sequence length of 250 base pairs (*74*, *76*). For each experiment and sequencing run, a shared community file and a phylotypes (genus-level grouping) file were generated using OTUs binned at 97% identity generated using the dist.seqs, cluster, make.shared, and classify.otu commands in mothur. OTU numbers were arbitrarily assigned in the binning process and are referred to throughout the manuscript in association with their most detailed level of taxonomy. Classification of OTUs was carried out using the mothur implementation of the Ribosomal Database Project (RDP) Classifier and the RDP taxonomy training set 14 (Trainset14_032015.rdp), available on the mothur website.

We performed microbial ecology analysis using the vegan package 2.2-1 and *mvabund* in R (*77*–*79*). For relative abundance and ordination analysis, samples were normalized to the percentage of total reads, and we restricted the analysis to OTUs that were present at greater than 1% of the sample population. All OTUs were included in diversity analysis. Direct community similarity comparisons were performed using the Bray-Curtis similarity index. We performed ordinations using principal components analysis on Hellinger-transformed normalized OTU tables generated using Euclidean distances (*80*). We determined the significance of differences in community composition using PERMANOVA (adonis) with 10,000 permutations using Euclidean distances. We performed all analyses in R and GraphPad Prism 6. We compared means via Student's *t* test (when normally distributed), Mann-Whitney *U* test (when non-Gaussian), and ANOVA with Holm-Sidak's multiple comparisons test as appropriate. Outliers were identified using the ROUT (Robust regression and Outlier Removal) method with a highly strict and previously defined false discovery rate of 0.1% (*81*). A single measurement in the germ-free oxygen exposure experiment (an IgM concentration in an oxygen-exposed germ-free mouse; Fig. 5A) and a single measurement in the ceftriaxone oxygen exposure experiment (an IgM concentration in an unexposed day 0 mouse; Fig. 6C) met this threshold and were excluded from analysis. Linear regressions between relative abundances and cytokine concentrations were performed using log-transformed cytokine concentrations.

SUPPLEMENTARY MATERIALS

stm.sciencemag.org/cgi/content/full/12/556/eaau9959/DC1
Fig. S1. Effects of acute hyperoxia on lung microbial communities.
Fig. S2. Correlations among lung and cecal bacterial communities and lung inflammation after hyperoxia.
Fig. S3. Hypothesized causal relationships and experimental approach.
Table S1. *mvabund* comparisons between lung bacterial taxa and lung cytokine concentrations.
Table S2. *mvabund* comparisons between cecal bacterial taxa and lung cytokine concentrations.
Data file S1. Individual-level data for all figures.

View/request a protocol for this paper from *Bio-protocol*.

REFERENCES AND NOTES

1. L. Frank, J. R. Bucher, R. J. Roberts, Oxygen toxicity in neonatal and adult animals of various species. *J. Appl. Physiol. Respir. Environ. Exerc. Physiol.* **45**, 699–704 (1978).
2. R. H. Kallet, M. A. Matthay, Hyperoxic acute lung injury. *Respir. Care* **58**, 123–141 (2013).
3. G. Matute-Bello, C. W. Frevert, T. R. Martin, Animal models of acute lung injury. *Am. J. Physiol. Lung Cell. Mol. Physiol.* **295**, L379–L399 (2008).
4. D. K. Chu, L. H.-Y. Kim, P. J. Young, N. Zamiri, S. A. Almenawer, R. Jaeschke, W. Szczeklik, H. J. Schünemann, J. D. Neary, W. Alhazzani, Mortality and morbidity in acutely ill adults treated with liberal versus conservative oxygen therapy (IOTA): A systematic review and meta-analysis. *Lancet* **391**, 1693–1705 (2018).
5. M. Girardis, S. Busani, E. Damiani, A. Donati, L. Rinaldi, A. Marudi, A. Morelli, M. Antonelli, M. Singer, Effect of conservative vs conventional oxygen therapy on mortality among patients in an intensive care unit: The oxygen-ICU randomized clinical trial. *JAMA* **316**, 1583–1589 (2016).
6. R. E. Barber, W. K. Hamilton, Oxygen toxicity in man. A prospective study in patients with irreversible brain damage. *N. Engl. J. Med.* **283**, 1478–1484 (1970).
7. J. Almirall, I. Bolibar, M. Serra-Prat, J. Roig, I. Hospital, E. Carandell, M. Agusti, P. Ayuso, A. Estela, A. Torres; Community-Acquired Pneumonia in Catalan Countries (PACAP) Study

Group, New evidence of risk factors for community-acquired pneumonia: A population-based study. *Eur. Respir. J.* **31**, 1274–1284 (2008).
8. S. Six, K. Jaffal, G. Ledoux, E. Jaillette, F. Wallet, S. Nseir, Hyperoxemia as a risk factor for ventilator-associated pneumonia. *Crit. Care* **20**, 195 (2016).
9. A. L. Lavoisier, Memoires de medecine et de physicque medicale. *Soc. Roy. de Medicine* **5**, 569 (1783).
10. J. Priestley, An account of further discoveries in air. By the Rev. Joseph Priestley, LL. D. F. R. S. in Letters to Sir John Pringle, Bart. P. R. S. and the Rev. Dr. Price, F. R. S. *Phil. Trans.* **65**, 384–394 (1775).
11. V. Bhandari, R. Choo-Wing, A. Harijith, H. Sun, M. A. Syed, R. J. Homer, J. A. Elias, Increased hyperoxia-induced lung injury in nitric oxide synthase 2 null mice is mediated via angiopoietin 2. *Am. J. Respir. Cell Mol. Biol.* **46**, 668–676 (2012).
12. H.-Y. Cho, A. E. Jedlicka, S. P. Reddy, L.-Y. Zhang, T. W. Kensler, S. R. Kleeberger, Linkage analysis of susceptibility to hyperoxia. Nrf2 is a candidate gene. *Am. J. Respir. Cell. Mol. Biol.* **26**, 42–51 (2002).
13. H. Clark, L. S. Clark, The genetics of neonatal respiratory disease. *Semin. Fetal Neonatal Med.* **10**, 271–282 (2005).
14. G. S. Whitehead, L. H. Burch, K. G. Berman, C. A. Piantadosi, D. A. Schwartz, Genetic basis of murine responses to hyperoxia-induced lung injury. *Immunogenetics* **58**, 793–804 (2006).
15. R. P. Dickson, J. R. Erb-Downward, F. J. Martinez, G. B. Huffnagle, The microbiome and the respiratory tract. *Annu. Rev. Physiol.* **78**, 481–504 (2016).
16. R. P. Dickson, J. R. Erb-Downward, N. R. Falkowski, E. M. Hunter, S. L. Ashley, G. B. Huffnagle, The lung microbiota of healthy mice are highly variable, cluster by environment, and reflect variation in baseline lung innate immunity. *Am. J. Respir. Crit. Care Med.* **198**, 497–508 (2018).
17. R. P. Dickson, J. R. Erb-Downward, C. M. Freeman, L. McCloskey, N. R. Falkowski, G. B. Huffnagle, J. L. Curtis, Bacterial topography of the healthy human lower respiratory tract. *mBio* **8**, e02287-16 (2017).
18. L. N. Segal, J. C. Clemente, J.-C. J. Tsay, S. B. Koralov, B. C. Keller, B. G. Wu, Y. Li, N. Shen, E. Ghedin, A. Morris, P. Diaz, L. Huang, W. R. Wikoff, C. Ubeda, A. Artacho, W. N. Rom, D. H. Sterman, R. G. Collman, M. J. Blaser, M. D. Weiden, Enrichment of the lung microbiome with oral taxa is associated with lung inflammation of a Th17 phenotype. *Nat. Microbiol.* **1**, 16031 (2016).
19. R. P. Dickson, F. J. Martinez, G. B. Huffnagle, The role of the microbiome in exacerbations of chronic lung diseases. *Lancet* **384**, 691–702 (2014).
20. M. Hilty, C. Burke, H. Pedro, P. Cardenas, A. Bush, C. Bossley, J. Davies, A. Ervine, L. Poulter, L. Pachter, M. F. Moffatt, W. O. C. Cookson, Disordered microbial communities in asthmatic airways. *PLOS ONE* **5**, e8578 (2010).
21. R. P. Dickson, B. H. Singer, M. W. Newstead, N. R. Falkowski, J. R. Erb-Downward, T. J. Standiford, G. B. Huffnagle, Enrichment of the lung microbiome with gut bacteria in sepsis and the acute respiratory distress syndrome. *Nat. Microbiol.* **1**, 16113 (2016).
22. R. P. Dickson, M. J. Schultz, T. van der Poll, L. R. Schouten, N. R. Falkowski, J. E. Luth, M. W. Sjoding, C. A. Brown, R. Chanderraj, G. B. Huffnagle, L. D. J. Bos, Lung microbiota predict clinical outcomes in critically ill patients. *Am. J. Respir. Crit. Care Med.* **201**, 555–563 (2020).
23. P. L. Molyneaux, M. J. Cox, S. A. Willis-Owen, P. Mallia, K. E. Russell, A.-M. Russell, E. Murphy, S. L. Johnston, D. A. Schwartz, A. U. Wells, W. O. C. Cookson, T. M. Maher, M. F. Moffatt, The role of bacteria in the pathogenesis and progression of idiopathic pulmonary fibrosis. *Am. J. Respir. Crit. Care Med.* **190**, 906–913 (2014).
24. D. N. O'Dwyer, S. L. Ashley, S. J. Gurczynski, M. Xia, C. Wilke, N. R. Falkowski, K. C. Norman, K. B. Arnold, G. B. Huffnagle, M. L. Salisbury, M. K. Han, K. R. Flaherty, E. S. White, F. J. Martinez, J. R. Erb-Downward, S. Murray, B. B. Moore, R. P. Dickson, Lung microbiota contribute to pulmonary inflammation and disease progression in pulmonary fibrosis. *Am. J. Respir. Crit. Care Med.* **199**, 1127–1138 (2019).
25. A. R. Panzer, S. V. Lynch, C. Langelier, J. D. Christie, K. McCauley, M. Nelson, C. K. Cheung, N. L. Benowitz, M. J. Cohen, C. S. Calfee, Lung microbiota is related to smoking status and to development of acute respiratory distress syndrome in critically ill trauma patients. *Am. J. Respir. Crit. Care Med.* **197**, 621–631 (2018).
26. A. Brune, P. Frenzel, H. Cypionka, Life at the oxic-anoxic interface: Microbial activities and adaptations. *FEMS Microbiol. Rev.* **24**, 691–710 (2000).
27. E. Cabiscol, J. Tamarit, J. Ros, Oxidative stress in bacteria and protein damage by reactive oxygen species. *Int. Microbiol.* **3**, 3–8 (2000).
28. F. Rivera-Chávez, C. A. Lopez, A. J. Bäumler, Oxygen as a driver of gut dysbiosis. *Free Radic. Biol. Med.* **105**, 93–101 (2017).
29. J. J. Wright, K. M. Konwar, S. J. Hallam, Microbial ecology of expanding oxygen minimum zones. *Nat. Rev. Microbiol.* **10**, 381–394 (2012).
30. D. J. Weber, W. A. Rutala, E. E. Sickbert-Bennett, G. P. Samsa, V. Brown, M. S. Niederman, Microbiology of ventilator-associated pneumonia compared with that of hospital-acquired pneumonia. *Infect. Control Hosp. Epidemiol.* **28**, 825–831 (2007).
31. R. Gaupp, N. Ledala, G. A. Somerville, Staphylococcal response to oxidative stress. *Front. Cell. Infect. Microbiol.* **2**, 33 (2012).
32. B. S. Scales, R. P. Dickson, G. B. Huffnagle, A tale of two sites: How inflammation can reshape the microbiomes of the gut and lungs. *J. Leukoc. Biol.* **100**, 943–950 (2016).
33. P. J. Barnes, Reactive oxygen species and airway inflammation. *Free Radic. Biol. Med.* **9**, 235–243 (1990).
34. T. J. Schuijt, J. M. Lankelma, B. P. Scicluna, F. de Sousa e Melo, J. J. Roelofs, J. D. de Boer, A. J. Hoogendijk, R. de Beer, A. de Vos, C. Belzer, W. M. de Vos, T. van der Poll, W. J. Wiersinga, The gut microbiota plays a protective role in the host defence against pneumococcal pneumonia. *Gut* **65**, 575–583 (2016).
35. L. J. Magnotti, J. S. Upperman, D. Z. Xu, Q. Lu, E. A. Deitch, Gut-derived mesenteric lymph but not portal blood increases endothelial cell permeability and promotes lung injury after hemorrhagic shock. *Ann. Surg.* **228**, 518–527 (1998).
36. D. Touati, Iron and oxidative stress in bacteria. *Arch. Biochem. Biophys.* **373**, 1–6 (2000).
37. E. S. Gollwitzer, S. Saglani, A. Trompette, K. Yadava, R. Sherburn, K. D. McCoy, L. P. Nicod, C. M. Lloyd, B. J. Marsland, Lung microbiota promotes tolerance to allergens in neonates via PD-L1. *Nat. Med.* **20**, 642–647 (2014).
38. A. P. Lauder, A. M. Roche, S. Sherrill-Mix, A. Bailey, A. L. Laughlin, K. Bittinger, R. Leite, M. A. Elovitz, S. Parry, F. D. Bushman, Comparison of placenta samples with contamination controls does not provide evidence for a distinct placenta microbiota. *Microbiome* **4**, 29 (2016).
39. T. X. Cui, B. Maheshwer, J. Y. Hong, A. M. Goldsmith, J. K. Bentley, A. P. Popova, Hyperoxic exposure of immature mice increases the inflammatory response to subsequent rhinovirus infection: Association with danger signals. *J. Immunol.* **196**, 4692–4705 (2016).
40. A. Trompette, E. S. Gollwitzer, K. Yadava, A. K. Sichelstiel, N. Sprenger, C. Ngom-Bru, C. Blanchard, T. Junt, L. P. Nicod, N. L. Harris, B. J. Marsland, Gut microbiota metabolism of dietary fiber influences allergic airway disease and hematopoiesis. *Nat. Med.* **20**, 159–166 (2014).
41. V. Poroyko, F. Meng, A. Meliton, T. Afonyushkin, A. Ulanov, E. Semenyuk, O. Latif, V. Tesic, A. A. Birukova, K. G. Birukov, Alterations of lung microbiota in a mouse model of LPS-induced lung injury. *Am. J. Physiol. Lung Cell. Mol. Physiol.* **309**, L76–L83 (2015).
42. R. P. Dickson, The microbiome and critical illness. *Lancet Respir. Med.* **4**, 59–72 (2016).
43. K. C. Barry, M. F. Fontana, J. L. Portman, A. S. Dugan, R. E. Vance, IL-1α signaling initiates the inflammatory response to virulent *Legionella pneumophila* in vivo. *J. Immunol.* **190**, 6329–6339 (2013).
44. L. A. Borthwick, The IL-1 cytokine family and its role in inflammation and fibrosis in the lung. *Semin. Immunopathol.* **38**, 517–534 (2016).
45. C. Li, P. Yang, Y. Sun, T. Li, C. Wang, Z. Wang, Z. Zou, Y. Yan, W. Wang, C. Wang, Z. Chen, L. Xing, C. Tang, X. Ju, F. Guo, J. Deng, Y. Zhao, P. Yang, J. Tang, H. Wang, Z. Zhao, Z. Yin, B. Cao, X. Wang, C. Jiang, IL-17 response mediates acute lung injury induced by the 2009 pandemic influenza A (H1N1) virus. *Cell Res.* **22**, 528–538 (2012).
46. G. U. Meduri, G. Kohler, S. Headley, E. Tolley, F. Stentz, A. Postlethwaite, Inflammatory cytokines in the BAL of patients with ARDS. Persistent elevation over time predicts poor outcome. *Chest* **108**, 1303–1314 (1995).
47. M. Miyamoto, O. Prause, M. Sjostrand, M. Laan, J. Lötvall, A. Linden, Endogenous IL-17 as a mediator of neutrophil recruitment caused by endotoxin exposure in mouse airways. *J. Immunol.* **170**, 4665–4672 (2003).
48. P. M. Suter, S. Suter, E. Girardin, P. Roux-Lombard, G. E. Grau, J. M. Dayer, High bronchoalveolar levels of tumor necrosis factor and its inhibitors, interleukin-1, interferon, and elastase, in patients with adult respiratory distress syndrome after trauma, shock, or sepsis. *Am. Rev. Respir. Dis.* **145**, 1016–1022 (1992).
49. J. F. Holter, J. E. Weiland, E. R. Pacht, J. E. Gadek, W. B. Davis, Protein permeability in the adult respiratory distress syndrome. Loss of size selectivity of the alveolar epithelium. *J. Clin. Invest.* **78**, 1513–1522 (1986).
50. C. M. Hendrickson, J. Abbott, H. Zhuo, K. D. Liu, C. S. Calfee, M. A. Matthay; NHLBI ARDS Network, Higher mini-BAL total protein concentration in early ARDS predicts faster resolution of lung injury measured by more ventilator-free days. *Am. J. Physiol. Lung Cell. Mol. Physiol.* **312**, L579–L585 (2017).
51. H. Deng, S. N. Mason, R. L. Auten Jr., Lung inflammation in hyperoxia can be prevented by antichemokine treatment in newborn rats. *Am. J. Respir. Crit. Care Med.* **162**, 2316–2323 (2000).
52. R. D. Sue, J. A. Belperio, M. D. Burdick, L. A. Murray, Y. Y. Xue, M. C. Dy, J. J. Kwon, M. P. Keane, R. M. Strieter, CXCR2 is critical to hyperoxia-induced lung injury. *J. Immunol.* **172**, 3860–3868 (2004).
53. R. P. Dickson, J. R. Erb-Downward, H. C. Prescott, F. J. Martinez, J. L. Curtis, V. N. Lama, G. B. Huffnagle, Intraalveolar catecholamines and the human lung microbiome. *Am. J. Respir. Crit. Care Med.* **192**, 257–259 (2015).
54. N. K. Nakagawa, M. L. Franchini, P. Driusso, L. R. de Oliveira, P. H. Saldiva, G. Lorenzi-Filho, Mucociliary clearance is impaired in acutely ill patients. *Chest* **128**, 2772–2777 (2005).
55. H. Wu, A. Kuzmenko, S. Wan, L. Schaffer, A. Weiss, J. H. Fisher, K. S. Kim, F. X. McCormack, Surfactant proteins A and D inhibit the growth of Gram-negative bacteria by increasing membrane permeability. *J. Clin. Invest.* **111**, 1589–1602 (2003).
56. H. D. Holland, The oxygenation of the atmosphere and oceans. *Philos. Trans. R. Soc. Lond. B Biol. Sci.* **361**, 903–915 (2006).

57. F. Rivera-Chavez, L. F. Zhang, F. Faber, C. A. Lopez, M. X. Byndloss, E. E. Olsan, G. Xu, E. M. Velazquez, C. B. Lebrilla, S. E. Winter, A. J. Baumler, Depletion of butyrate-producing *Clostridia* from the gut microbiota drives an aerobic luminal expansion of *Salmonella*. *Cell Host Microbe* **19**, 443–454 (2016).
58. H. Kanafani, S. E. Martin, Catalase and superoxide dismutase activities in virulent and nonvirulent *Staphylococcus aureus* isolates. *J. Clin. Microbiol.* **21**, 607–610 (1985).
59. M. H. Karavolos, M. J. Horsburgh, E. Ingham, S. J. Foster, Role and regulation of the superoxide dismutases of *Staphylococcus aureus*. *Microbiology* **149**, 2749–2758 (2003).
60. B. Park, V. Nizet, G. Y. Liu, Role of *Staphylococcus aureus* catalase in niche competition against *Streptococcus pneumoniae*. *J. Bacteriol.* **190**, 2275–2278 (2008).
61. V. L. Goncalves, L. S. Nobre, J. B. Vicente, M. Teixeira, L. M. Saraiva, Flavohemoglobin requires microaerophilic conditions for nitrosative protection of *Staphylococcus aureus*. *FEBS Lett.* **580**, 1817–1821 (2006).
62. O. Uziel, I. Borovok, R. Schreiber, G. Cohen, Y. Aharonowitz, Transcriptional regulation of the *Staphylococcus aureus* thioredoxin and thioredoxin reductase genes in response to oxygen and disulfide stress. *J. Bacteriol.* **186**, 326–334 (2004).
63. C. Dahlgren, A. Karlsson, Respiratory burst in human neutrophils. *J. Immunol. Methods* **232**, 3–14 (1999).
64. H. J. Forman, M. Torres, Reactive oxygen species and cell signaling: Respiratory burst in macrophage signaling. *Am. J. Respir. Crit. Care Med.* **166**, S4–S8 (2002).
65. D. N. O'Dwyer, X. Zhou, C. A. Wilke, M. Xia, N. R. Falkowski, K. C. Norman, K. B. Arnold, G. B. Huffnagle, S. Murray, J. R. Erb-Downward, G. A. Yanik, B. B. Moore, R. P. Dickson, Lung dysbiosis, inflammation, and injury in hematopoietic cell transplantation. *Am. J. Respir. Crit. Care Med.* **198**, 1312–1321 (2018).
66. R. P. Dickson, J. R. Erb-Downward, H. C. Prescott, F. J. Martinez, J. L. Curtis, V. N. Lama, G. B. Huffnagle, Analysis of culture-dependent versus culture-independent techniques for identification of bacteria in clinically obtained bronchoalveolar lavage fluid. *J. Clin. Microbiol.* **52**, 3605–3613 (2014).
67. N. Reamaroon, M. W. Sjoding, K. Lin, T. J. Iwashyna, K. Najarian, Accounting for label uncertainty in machine learning for detection of acute respiratory distress syndrome. *IEEE J. Biomed. Health Inform.* **23**, 407–415 (2018).
68. P. D. Bozyk, J. K. Bentley, A. P. Popova, A. C. Anyanwu, M. D. Linn, A. M. Goldsmith, G. S. Pryhuber, B. B. Moore, M. B. Hershenson, Neonatal periostin knockout mice are protected from hyperoxia-induced alveolar simplication. *PLOS ONE* **7**, e31336 (2012).
69. V. Ratner, A. Starkov, D. Matsiukevich, R. A. Polin, V. S. Ten, Mitochondrial dysfunction contributes to alveolar developmental arrest in hyperoxia-exposed mice. *Am. J. Respir. Cell Mol. Biol.* **40**, 511–518 (2009).
70. K. L. Mason, J. R. Erb Downward, K. D. Mason, N. R. Falkowski, K. A. Eaton, J. Y. Kao, V. B. Young, G. B. Huffnagle, *Candida albicans* and bacterial microbiota interactions in the cecum during recolonization following broad-spectrum antibiotic therapy. *Infect. Immun.* **80**, 3371–3380 (2012).
71. S. J. Salter, M. J. Cox, E. M. Turek, S. T. Calus, W. O. Cookson, M. F. Moffatt, P. Turner, J. Parkhill, N. J. Loman, A. W. Walker, Reagent and laboratory contamination can critically impact sequence-based microbiome analyses. *BMC Biol.* **12**, 87 (2014).
72. J. G. Caporaso, C. L. Lauber, W. A. Walters, D. Berg-Lyons, C. A. Lozupone, P. J. Turnbaugh, N. Fierer, R. Knight, Global patterns of 16S rRNA diversity at a depth of millions of sequences per sample. *Proc. Natl. Acad. Sci. U.S.A.* **108** (Suppl. 1), 4516–4522 (2011).
73. J. J. Kozich, S. L. Westcott, N. T. Baxter, S. K. Highlander, P. D. Schloss, Development of a dual-index sequencing strategy and curation pipeline for analyzing amplicon sequence data on the MiSeq Illumina sequencing platform. *Appl. Environ. Microbiol.* **79**, 5112–5120 (2013).
74. P. D. Schloss, MiSeq SOP (mothur, 2015); http://www.mothur.org/wiki/MiSeq_SOP.
75. M. A. Sze, M. Abbasi, J. C. Hogg, D. D. Sin, A comparison between droplet digital and quantitative PCR in the analysis of bacterial 16S load in lung tissue samples from control and COPD GOLD 2. *PLOS ONE* **9**, e110351 (2014).
76. P. D. Schloss, S. L. Westcott, T. Ryabin, J. R. Hall, M. Hartmann, E. B. Hollister, R. A. Lesniewski, B. B. Oakley, D. H. Parks, C. J. Robinson, J. W. Sahl, B. Stres, G. G. Thallinger, D. J. Van Horn, C. F. Weber, Introducing mothur: Open-source, platform-independent, community-supported software for describing and comparing microbial communities. *Appl. Environ. Microbiol.* **75**, 7537–7541 (2009).
77. J. Oksanen, F. G. Blanchet, M. Friendly, R. Kindt, P. Legendre, D. McGlinn, P. R. Minchin, R. B. O'Hara, G. L. Simpson, P. Solymos, M. H. H. Stevens, E. Szoecs, H. Wagner, vegan: Community Ecology Package (2019); https://CRAN.R-project.org/package=vegan.
78. R Core Team, R: A language and environment for statistical computing (R Foundation for Statistical Computing, Vienna, Austria, 2019); https://www.R-project.org/.
79. Y. Wang, U. Naumann, S. T. Wright, D. I. Warton, mvabund—An R package for model-based analysis of multivariate abundance data. *Methods Ecol. Evol.* **3**, 471–474 (2012).
80. P. Legendre, E. D. Gallagher, Ecologically meaningful transformations for ordination of species data. *Oecologia* **129**, 271–280 (2001).
81. H. J. Motulsky, R. E. Brown, Detecting outliers when fitting data with nonlinear regression - a new method based on robust nonlinear regression and the false discovery rate. *BMC Bioinformatics* **7**, 123 (2006).

Acknowledgments: We thank K. Eaton for expertise in the design and execution of our germ-free murine experiments, C. Brown for informatics assistance, and S. Garantziotis for helpful comments. **Funding:** Funding was provided by the NIH through grant numbers T32HL007517 (to S.L.A.), K23HL109149 (to A.P.P.), R01HL140572 (to A.P.P.), K23HL130641 (to R.P.D.), R21AI137669 (to R.P.D.), R01HL144599 (to R.P.D.), R01HL121774 (to G.B.H.), K01HL136687 (to M.W.S.), and R01GM099549 (to T.M.S.). The content of this study is solely the responsibility of the authors and does not necessarily represent the official views of the NIH. Support was provided by the Host Microbiome Initiative of the University of Michigan and the Michigan Center for Integrative Research in Critical Care. **Author contributions:** S.L.A., A.P.P., T.X.C., M.J.H., T.M.S., W.R.B., M.G.D., N.R.F., J.M.B., K.J.H., and R.P.D. designed and performed murine experiments. M.W.S. and R.P.D. designed and performed experimental analysis of human data. S.L.A., A.P.P., T.X.C., J.M.B., J.R.E.-D., G.B.H., and R.P.D. analyzed murine data. M.W.S. and R.P.D. analyzed human data. S.L.A., M.W.S., A.P.P., T.M.S., J.R.E.-D., G.B.H., and R.P.D. provided critical analysis and discussion. S.L.A. wrote the first draft, and all authors participated in revision of the manuscript. **Competing interests:** The authors declare that they have no competing interests. **Data and materials availability:** All data associated with this study are present in the paper or the Supplementary Materials. Bacterial sequences are available in the NCBI Sequence Read Archive (accession numbers PRJNA545314, PRJNA545329, PRJNA545477, and PRJNA545494). Bacterial culture results, OTU tables, taxonomy classification tables, and experimental metadata tables are available at https://github.com/dicksonlunglab/hyperoxia_lung_microbiome.

Submitted 7 September 2018
Resubmitted 14 June 2019
Accepted 21 January 2020
Published 12 August 2020
10.1126/scitranslmed.aau9959

Citation: S. L. Ashley, M. W. Sjoding, A. P. Popova, T. X. Cui, M. J. Hoostal, T. M. Schmidt, W. R. Branton, M. G. Dieterle, N. R. Falkowski, J. M. Baker, K. J. Hinkle, K. E. Konopka, J. R. Erb-Downward, G. B. Huffnagle, R. P. Dickson, Lung and gut microbiota are altered by hyperoxia and contribute to oxygen-induced lung injury in mice. *Sci. Transl. Med.* **12**, eaau9959 (2020).

Science Translational Medicine

Lung and gut microbiota are altered by hyperoxia and contribute to oxygen-induced lung injury in mice

Shanna L. Ashley, Michael W. Sjoding, Antonia P. Popova, Tracy X. Cui, Matthew J. Hoostal, Thomas M. Schmidt, William R. Branton, Michael G. Dieterle, Nicole R. Falkowski, Jennifer M. Baker, Kevin J. Hinkle, Kristine E. Konopka, John R. Erb-Downward, Gary B. Huffnagle and Robert P. Dickson

Sci Transl Med **12**, eaau9959.
DOI: 10.1126/scitranslmed.aau9959

Linking hyperoxia to microbial dysbiosis

Inhaled oxygen is a commonly administered therapy that causes severe lung injury in animals and is associated with poor clinical outcomes in humans. The bacteria that live within the body's lungs and gut are highly variable in their tolerance of oxygen. Ashley *et al.* now report that in both humans and mice, inhaled oxygen influenced respiratory bacterial communities. In mice, variations in lung and gut bacterial communities correlated with the severity of lung injury, and germ-free mice were protected from oxygen-induced lung injury. These results suggest that the bacteria of our lungs and gut play an important role in the pathogenesis of oxygen-induced lung injury.